# Electron Temperature Fluctuations During Magnetic Reconnection in the Reversed-Field Pinch

by

Cale P. Kasten

Undergraduate thesis submitted in partial fulfillment of the requirements for the degree of

Bachelor of Science

(Engineering Physics)

at the

UNIVERSITY OF WISCONSIN - MADISON

April 5, 2011

*The University of Wisconsin – Madison*
*Department of Engineering Physics*

*Candidate for the degree of* ***Bachelor of Science***

***Engineering Physics***

*For:* **Spring 2011**

## Cale Phillip Kasten

*The undersigned report that a research thesis was completed and defended on* April 5, 2011.

*Thesis title*: Electron temperature fluctuations during magnetic reconnection in the reversed-field pinch.

*in partial fulfillment of the requirements for the* ***Bachelor of Science: Engineering Physics*** *Degree and the* ***Undergraduate Honors in Research*** *designation.*

| Committee Members Names | Signature of Committee Members |
|---|---|
| **Sovinec, Carl R.** | Carl Sovinec |
| **Den Hartog, Daniel J.** | Daniel J. Den Hartog |
| **Hegna, Christopher C.** | Chris Hegna |
| | |
| | |

# Abstract

Electron temperature correlates to the dominant $m = 0, n = 1$ edge-resonant tearing mode during sawtooth events in the Madison Symmetric Torus reversed-field pinch. Using a high-repetition-rate Thomson scattering diagnostic, electron temperature measurements are taken at 21 radial locations at a 25 kHz repetition rate, on the same order as the tearing mode rotation frequency. Immediately prior to the sawtooth a toroidal edge electron temperature structure forms, creating a heat-confining island. During the sawtooth the behavior of the edge structure changes to an isothermal island. Also during the sawtooth when the $m = 0, n = 1$ mode amplitude is largest, there is a core electron temperature fluctuation correlated to the edge-resonant magnetic mode. It is speculated that the core temperature fluctuation arises from the finite core $m = 0, n = 1$ radial eigenfunction and finite core $m = 1$ modes. The core $m = 0, n = 1$ correlated fluctuations may also have an effect on overall core electron temperature confinement by reducing the edge temperature gradient. The fluctuation analysis was also performed for the $m = 0, n = 2$ mode and for $m = 0$ bursts in improved confinement plasmas, but no definitive results were obtained.

# Acknowledgements

There are several people without whom this work could not have been completed. In particular, I need to thank my adviser, Dr. Daniel Den Hartog, for his guidance and patience. Former graduate student Hillary Stephens conducted the initial work on electron temperature fluctuations in the MST, and without her results and IDL code framework this thesis would not be possible. I have relied on the expertise and experience of graduate students Joshua Reusch and Eli Parke to develop a baseline understanding of experimental plasma physics. I also need to thank the members of the Thomson scattering group and the MST research group. Without them the MST and Thomson scattering simply would not operate.

# Contents

# List of Figures

# List of Tables

# 1 Introduction

Fusion reactions have the potential to provide vast amounts of clean, safe energy to the increasingly energy-dependent world. To initiate a fusion reaction, the reactant nuclei must be confined together at high density and temperature [1]. Several methods have been proposed and tested to achieve the proper confinement conditions. The most advanced method is magnetically confining and heating a plasma of reactants. Since the reactant nuclei are charged, they feel forces due to electric and magnetic fields. By manipulating the fields the particles can be confined and heated. The study of electron energy confinement and transport within the plasma is important because electrons play a large role in heating fusion reactants. This thesis examines the effects of electron temperature fluctuations on overall electron temperature confinement in reversed-field pinch plasmas.

## 1.1 The Reversed-Field Pinch

The reversed-field pinch (RFP) is a type of toroidal[1] magnetic confinement device used to study plasma physics relevant to fusion energy research. The magnetic configuration of an RFP is usually described using force-free magnetohydrodynamic (MHD) modeling [2]. The force balance equation is given by

$$\vec{J} \times \vec{B} = \nabla P \tag{1}$$

[1]See Appendix A for a description of toroidal geometry and coordinates.

where $\vec{J}$, $\vec{B}$, and $P$ are the plasma current density, magnetic field, and plasma pressure, respectively. In force-free modeling $\nabla P$ is taken to be zero, allowing a simple analytic solution of the MHD equations.

Using Ampere's Law,

$$\nabla \times \vec{B} = \mu_0 \vec{J} \tag{2}$$

we find that,

$$\left(\nabla \times \vec{B}\right) \times \vec{B} = 0. \tag{3}$$

This equation is satisfied if the curl of $\vec{B}$ lies along $\vec{B}$, or:

$$\nabla \times \vec{B} = \lambda(r)\vec{B} \tag{4}$$

where $\lambda$ is a scalar function of the minor radius. If the assumption is made that $\lambda$ is a constant, the solution of equation 4 is,

$$\begin{aligned} B_\phi(r) &= B_{\phi 0} J_0(\lambda r) \\ B_\theta(r) &= B_{\theta 0} J_1(\lambda r). \end{aligned} \tag{5}$$

Here, $J_0$ and $J_1$ are Bessel functions of the first kind, $B_\phi$ is the toroidal magnetic field, and $B_\theta$ is the poloidal magnetic field. The resulting magnetic field equilibrium configuration is shown in figure 1, and matches fairly well with the experimentally measured equilibrium fields. Several RFP characteristics are predicted by this so-called "Bessel Function Model." The first is that the toroidal magnetic field reverses direction near the plasma edge, giving the name "reversed-field pinch." The second is that the toroidal and poloidal magnetic fields are comparable in magnitude everywhere except in the geometric center and near the plasma edge.

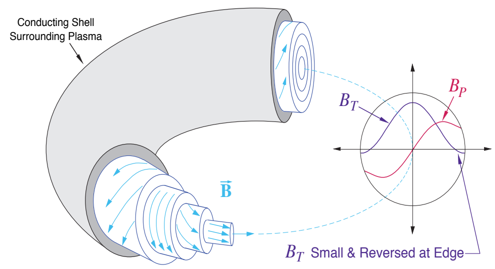


**Figure 1: Equilibrium magnetic field components of a RFP.** The toroidal field, $B_T$, reverses sign near the plasma edge and is comparable in magnitude to the poloidal field, $B_P$. Graphic courtesy of J. Sarff.

## 1.2 Tearing Modes and Sawtooth Events

As in any real-world experiment, small perturbations exist due to thermal effects. Non-uniformities in plasma current density and pressure create free energy which can destabilize perturbations. The perturbations studied in this thesis are magnetic tearing modes which can become unstable at specific radii in the plasma known as "resonant surfaces." They can experience rapid growth when magnetic field lines tear and reconnect, changing the magnetic topology of the plasma [3]. The locations of resonant surfaces are found by decomposing a small perturbation into Fourier harmonics,

$$\vec{k} = \frac{m}{r}\hat{\theta} - \frac{n}{R}\hat{\phi}. \tag{6}$$

Here, $\vec{k}$ is the wavenumber vector of the instability, $m$ and $n$ are the poloidal and toroidal mode numbers, $r$ is the minor radial coordinate, and $R$ is the major radius of the RFP. (This equation has been applied to the Madison Symmetric Torus RFP which employs a left-handed coordinate system, making $\hat{\phi}$ negative.)

If a perturbation has a component perpendicular to the magnetic field it will act to bend a magnetic field line. When a field line bends there is a strong restoring force due to magnetic tension that quickly stabilizes the perturbation. However, if the perturbation is parallel to the magnetic field the resulting force does not bend the field line. This condition is met when the wavenumber vector of the perturbation is perpendicular to the magnetic field (making the perturbation itself parallel to the field). Mathematically,

$$\vec{k} \cdot \vec{B} = 0 \tag{7}$$

or,

$$\frac{m}{r_s}B_\theta - \frac{n}{R}B_\phi = 0 \tag{8}$$

where $r_s$ is the location of the resonant surface of the $(m, n)$ tearing mode. Tearing modes can therefore become unstable when

$$\frac{m}{n} = \frac{r_s B_\phi}{R B_\theta}. \tag{9}$$

The right hand side of equation 9 is a common quantity in fusion energy research describing the amount of twist or helicity of the magnetic field lines. It is called the safety factor, $q$,

$$q(r) = \frac{rB_\phi}{RB_\theta} \tag{10}$$

A generic RFP q-profile is shown in figure 2. Locations where the q-profile takes on rational values given by $m/n$ are the expected locations of tearing modes.

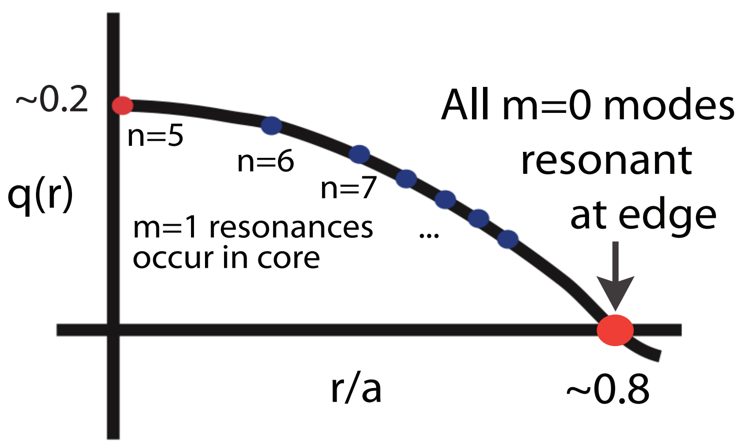


**Figure 2: q-profile showing the locations of resonant tearing modes.** All $m = 0$ tearing modes are resonant at the reversal surface where $B_\phi = 0$. The $m = 1, n = 5$ mode may come into resonance briefly after plasma phenomena known as sawtooth events.

Tearing modes non-linearly interact and grow during phenomena called sawtooth events. Sawtooth events are quasi-periodic relaxation events where the plasma moves to a lower energy state while approximately conserving global magnetic helicity [3, 4]. The mechanism driving the process begins with the externally applied toroidal electric field. The field preferentially drives parallel current in the core of the plasma. The higher current heats the core plasma, and since the plasma resistivity has an inverse dependence on temperature [5], the resistivity is lowered in the core. The lower plasma resistivity further increases parallel current in the core, creating a gradient in the parallel current density profile. The gradient supplies free energy to drive instabilities including tearing modes. Tearing modes are said to be "current-gradient driven."

Tearing mode instabilities do not only exist at resonant surfaces. They have finite radial extent due to a trade-off between magnetic tension restoring forces and the free energy available away from resonant surfaces. During sawtooth events these modes grow and eventually begin to overlap, creating a stochastic magnetic field and driving large $m = 0$ tearing mode growth [3]. The crash-phase of the sawtooth event occurs when magnetic field lines tear and reconnect, redistributing the peaked parallel current density by driving edge current [6]. The electron temperature profile is flattened in the core [7], and the redistribution of the parallel current density reduces the amount of free energy available to drive tearing mode instabilities. The process then restarts, with the externally applied toroidal electric field preferentially driving parallel current in the core.

The Madison Symmetric Torus (MST) [8] is a reversed-field pinch plasma physics experiment relevant to magnetically confined fusion energy research. The device consists of a hollow, 5 cm thick aluminum torus which serves as a stabilizing vacuum vessel. The vacuum vessel has major radius $R_0 = 1.5$ m and minor radius $a = 0.52$ m. Inside the vacuum vessel at the wall are magnetic field pick-up coils which measure magnetic field strength, phase, and phase velocity. By decomposing the measured signals into Fourier components, different magnetic modes can be resolved up to $n = 32$ [9]. Attached externally to the device are a variety of diagnostics, including a multi-point, multi-pulse Thomson scattering diagnostic for electron temperature measurements.

## 1.3 Thomson Scattering

Electron temperature measurements are taken with a multi-point, multi-pulse Thomson scattering diagnostic [10]. Thomson scattering on MST currently consists of two lasers which pulse light vertically through the MST vacuum chamber. The laser light is linearly-polarized in the toroidal direction. An electron feels a Lorentz force from the polarized laser pulse and radiates light with a temperature- and density-dependent wavelength shift [11]. After scattering off plasma electrons, the light from 21 radial locations is collected with fiber optic bundles (see figure 3).

The optical signal from each radial location is separated into several wavelength bands using four- or eight-channel polychromators and then converted into a voltage signal using an avalanche photodiode. The voltage signal is then amplified and digitized. A fitting routine integrates the voltage signal and converts the integral into the number of scattered photons using calibration data [12]. The data from separated wavelengths is recombined to give the measured relative Thomson scattering spectrum. An optimization routine [13] fits the measured spectrum to the theoretical spectrum given by the Selden equation [14], returning the absolute electron temperature and relative electron density.

The Thomson scattering lasers can be operated at a variety of effective data collection rates ranging from 2 kHz to 25 kHz. Fluctuation measurements were made using the 25 kHz "pulse-burst" operation [15] shown in figure 4. In this mode, each

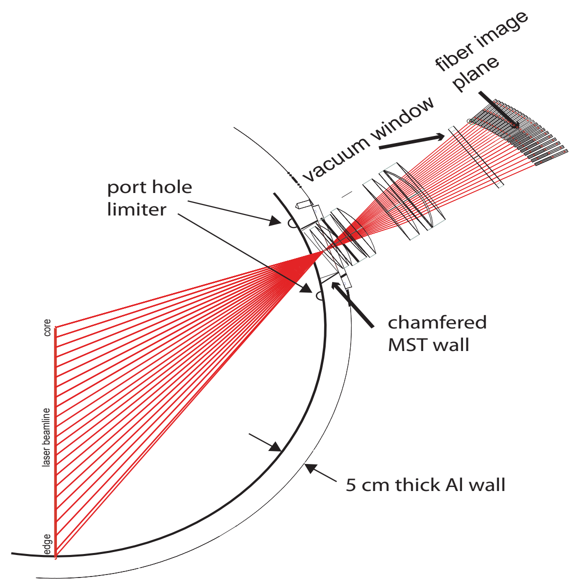


**Figure 3: Scattered light collection system.** Laser light enters the vacuum chamber vertically, scatters off plasma electrons, and is then collected at 21 radial locations with fiber optic cables. Graphic courtesy of J. Reusch [10].

laser fires 15 times per plasma discharge in five bursts of three pulses. The pulses from both lasers are interleaved so there are six total laser pulses in a single pulse-burst with 40 $\mu$s between each pulse, giving an overall data collection rate of 25 kHz. Consecutive pulse-bursts are separated by about 1 ms.

## 1.4 Key Results

In this thesis, electron temperature measurements are correlated to toroidally-rotating tearing mode instabilities in 400 kA standard plasmas in the MST RFP. The major result of the correlation analysis is that between 0 $\mu$s and 150 $\mu$s relative to the sawtooth event, the electron temperature becomes correlated to the edge-resonant $m = 0, n = 1$ magnetic mode across the entire minor diameter of the plasma. This is an important result because it shows that the tearing mode of interest, which is largest

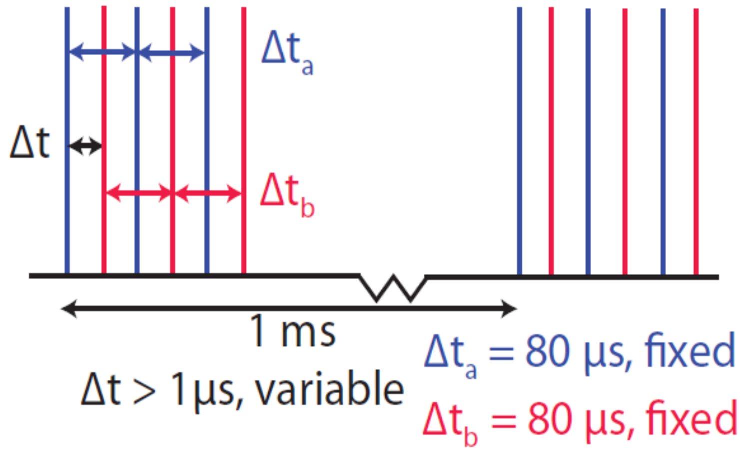


**Figure 4: Pulse-burst operation of Spectron lasers.** Each laser is fired three times in quick succession, separated by 80 $\mu$s. By interleaving the lasers as shown, a 25 kHz effective data collection rate is achieved. The burst of pulses is repeated five times per plasma discharge, giving 30 total electron temperature profile measurements per discharge. Graphic courtesy of H. Stephens [16].

near the *edge* of the plasma, has a dramatic effect on the *core* electron temperature during sawtooth events. Two possible explanations are explored. First, large $m = 1$ core tearing modes could interact to yield the $m = 0, n = 1$ behavior of the observed temperature fluctuation. Second, the $m = 0, n = 1$ radial eigenfunction is finite near the core of the plasma, making it possible for the mode to perturb the core during sawtooth events.

Another result of this work is that prior to the sawtooth event, an edge electron temperature fluctuation is observed near the resonant surface of the $m = 0, n = 1$ tearing mode. The fluctuation creates a heat-confining island. During the sawtooth the behavior of the island changes to isothermal. Using electron temperature fluctuation measurements, the location of the $m = 0, n = 1$ resonant surface is approximated. The resonant surface is found to lie well inside of the expected location found from an equilibrium reconstruction code. This may indicate that the equilibrium reconstruction is not correctly describing the plasma, or is not valid during sawtooth events. Limitations in the radial resolution of the Thomson scattering diagnostic near the plasma edge demand further investigation into $m = 0, n = 1$ correlated electron temperature fluctuations to determine the validity of the measurements.

The core electron temperature fluctuation is shown to have a large effect on overall core confinement. Core fluctuations link up well with highly resolved ensemble-averaged electron temperature evolution. At the sawtooth, the edge temperature gradient fluctuates toroidally and is therefore reduced and enhanced at certain locations. The core temperature at the reduced point is approximately constant at a low value while the temperature at the enhanced region drops with the ensemble-averaged core temperature. Once the ensemble-averaged temperature reaches 200 eV it stops decreasing and the core electron temperature fluctuation vanishes. This is evidence that the $m = 0, n = 1$ magnetic mode plays a role in core confinement.

The analysis was also performed for the $m = 0, n = 2$ mode in standard plasmas and small electron temperature fluctuations were found. During the sawtooth, the fluctuations have the opposite sign of the $m = 0, n = 1$ correlated fluctuations but are non-zero. The analysis was attempted for small $m = 0$ bursts in low current improved confinement plasmas, but lack of data limited the ability to draw conclusions about the effect of these events on the electron temperature.

## 1.5 Thesis Overview

This thesis is presented in the following way. Section 2 describes previous work on electron temperature fluctuations correlated to $m = 1$ tearing modes. Information about these modes motivates the study of $m = 0$ correlated fluctuations, and also allows analogies to be drawn between the $m = 0$ and $m = 1$ correlated fluctuations. Section 2 also describes the results of detailed magnetic measurements of the $m = 0, n = 1 - 4$ modes through the sawtooth cycle, giving important information about the mode structure for analysis of electron temperature fluctuations. Section 3 describes the model used for electron temperature fluctuation analysis and the Bayesian statistical process used to correlate Thomson scattering data to magnetic phase information. Limitations of the analysis and the results of the correlations are discussed in Section 4, and conclusions and suggestions for future work are outlined in Section 5.

Appendix A contains a description of toroidal geometry and coordinates for those not familiar with fusion energy devices. Appendices B and C provide a complete set of figures from the $m = 0, n = 1$ and the $m = 0, n = 2$ correlated fluctuations.

# 2 Previous Work

This section describes previous work done with electron temperature fluctuations correlated to the $m = 1, n = 5-8$ magnetic modes. Also, detailed magnetic measurements of the $m = 0, n = 1$ mode structure through the sawtooth cycle are presented.

## 2.1 Correlated $T_e$ Fluctuations in Standard Plasmas

Recently, electron temperature measurements were correlated to the $m = 1, n = 5-8$ magnetic tearing modes in 400 kA standard RFP plasmas [16, 17]. Since these are $m = 1$ modes, the poloidal phase of the mode was used for correlation. The model used to determine the electron temperature fluctuations assumes that the temperature fluctuation is in phase with the magnetic mode of interest. It is given by,

$$T_e = T_{e0,m,n} + \tilde{T}_{e,m,n} \cos(\theta_{m,n}). \quad (11)$$

Here, $T_e$ is the model electron temperature, $T_{e0,m,n}$ is a mean or background component, and $\tilde{T}_{e,m,n}$ is the fluctuating component of the electron temperature in phase with the magnetic mode, $\theta_{m,n}$.

The $m = 1$ tearing modes have resonant surfaces in the core of MST, as shown in the q-profile (figure 2). Therefore, two types of poloidal structures are possible in the core of MST with this model. The first is a localized flattening of the electron temperature profile, and the other is a localized peaking of the temperature profile. Each type of model is represented pictorially in figure 5.

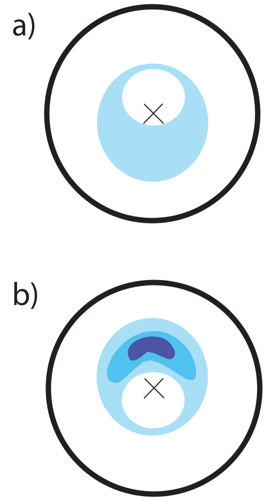


**Figure 5: Representation of possible $m = 1$ fluctuations.** Shown here are a) an isothermal island and b) a heat-confining island, in a poloidal cross-section of the MST. The X denotes the geometric axis. Graphic courtesy of H. Stephens [16].

Far away in time from sawtooth events, the dominant magnetic tearing mode is the $m = 1, n = 6$ mode. The results of the analysis show a fluctuation amplitude that is negative in the core and positive further out (see figure 6a). The result is a flattening of the electron temperature profile at the O-point of the mode ($\theta_{1,6} = 0$, the right side of figure 6b), and a sharpening of the profile at the X-point ($\theta_{1,6} = \pi$, the left side of figure 6b). This is indicative of an isothermal island as in figure 5a.

The radial location where the temperature fluctuation amplitudes change sign is interpreted as the location of the resonant surface of the $m = 1, n = 6$ tearing mode [16]. The same analysis was conducted for the $m = 1, n = 7$ mode as well. The locations of the resonant surfaces can be compared to the expected locations given by the q-profile found from the equilibrium reconstruction code MSTFit. A plot of the

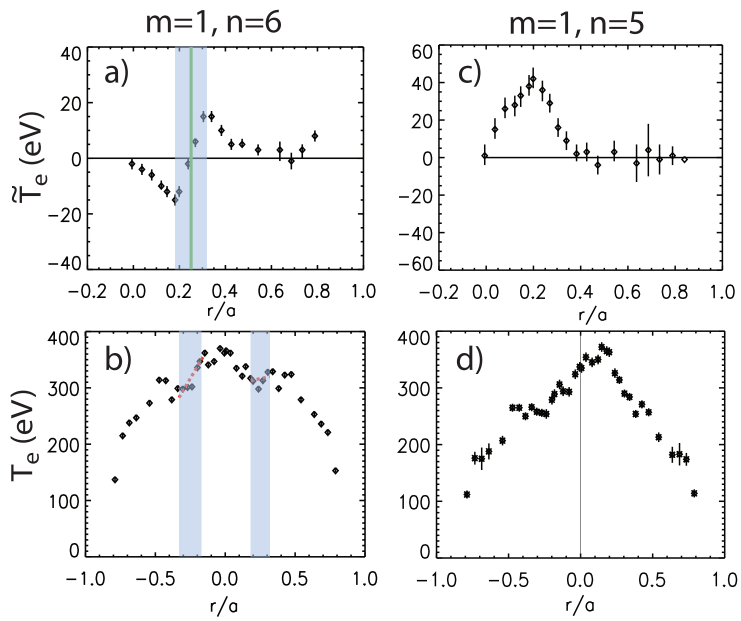


**Figure 6: Fluctuations and profiles correlated to $m = 1$ modes away from sawtooth.** The $m = 1, n = 6$ fluctuation amplitudes (a) exhibit a sign flip across the minor radius which acts to locally flatten the temperature profile (b) at the O-point. The $m = 1, n = 5$ fluctuation amplitudes (c) have the same sign across the minor radius which creates an off-axis peak in the temperature profile (d) at the O-point. Graphic courtesy of Hillary Stephens [16].

reconstructed q-profile is shown in figure 7. The red points are the radial locations of the $m = 1, n = 6-7$ resonant surfaces as measured from electron temperature fluctuation analysis, and the black points are the locations on the reconstructed q-profile (dashed line) representing the resonant surfaces. The locations of the resonant surfaces as measured by Thomson scattering data occur closer to the core of MST than in the equilibrium reconstruction.

Half a millisecond after a sawtooth event, the dominant tearing mode becomes the $m = 1, n = 5$ mode. In this case, the temperature fluctuation amplitudes are the

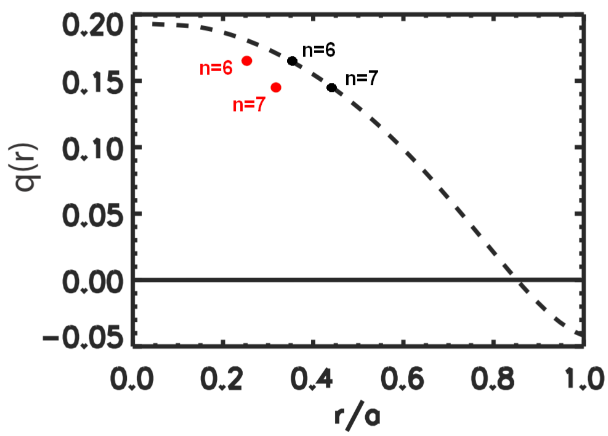


**Figure 7: Reconstructed q-profile with $T_e$ fluctuation-measured resonant surfaces.** The red points are the radial locations of the $m = 1, n = 6 - 7$ resonant surfaces as measured by fluctuation analysis of Thomson scattering data. The black points are the locations on the reconstructed q-profile (dashed line) which represent the resonant surfaces of the modes. Graphic adapted from H. Stephens' Ph.D thesis [16].

same sign in the core of the device. This type of fluctuation creates an an off-axis peak in the electron temperature profile (see figure 6c-d). This can also be interpreted as a heat-confining island rotating poloidally in the MST.

During the sawtooth event, both the $m = 1, n = 6$ and the $m = 1, n = 5$ correlated temperature fluctuations vanish. Figure 8 shows the $m = 1, n = 6$ correlated fluctuations at several time points relative to the sawtooth event. They vanish during the event and reappear about a millisecond after the sawtooth crash. The $m = 1, n = 5$ correlated fluctuations only appear half a millisecond after the sawtooth crash. Figure 9 shows the ensemble-averaged tearing mode amplitudes through the sawtooth cycle. The $m = 0$ mode is much larger than the $m = 1$ modes during the sawtooth event when the $m = 1$ correlated $T_e$ fluctuations are vanishing.

The lack of correlated temperature fluctuations with $m = 1$ modes during the saw-

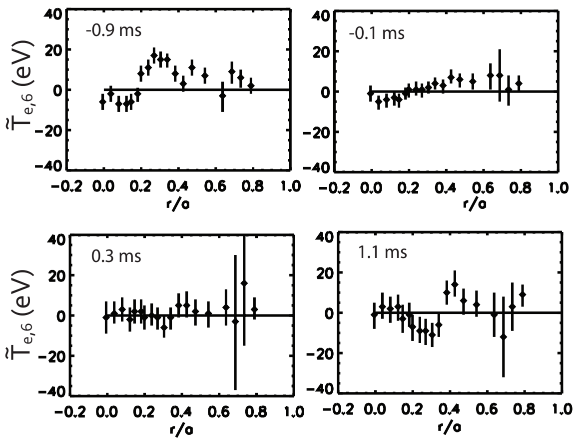


**Figure 8: Fluctuations correlated to $m = 1, n = 6$ through sawtooth.** The fluctuation amplitudes vanish through the sawtooth cycle, indicating that the $m = 1, n = 6$ mode no longer has the dominant effect on the electron temperature fluctuations. Graphic courtesy of Hillary Stephens [16].

tooth crash, combined with the observed $m = 0$ mode growth, leads to the following hypothesis: The dominant $m = 0$ mode has the most influential effect on the electron temperature during the sawtooth as it grows and dominates the mode spectrum. To test this, a fluctuation analysis similar to the one performed for $m = 1$ modes is performed for the $m = 0, n = 1$ tearing mode. As this thesis will show, during the sawtooth event electron temperature fluctuations become correlated to this mode. Fluctuations occur both at the edge of the plasma where the mode is resonant and in the core of the MST.

To make sense of the fluctuation results, something must be known about the structure of the $m = 0$ modes during sawtooth events. The next part of this section summarizes detailed magnetic measurements which provide a qualitative description

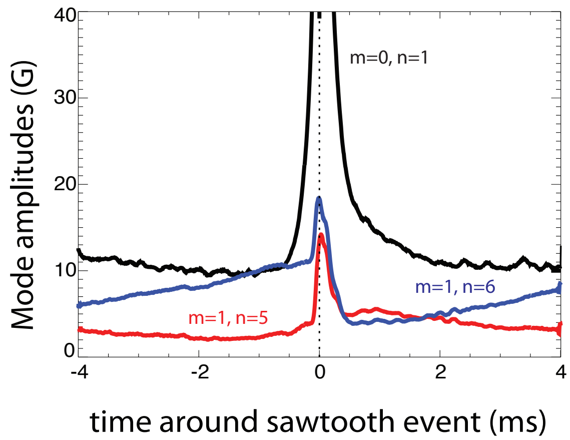


**Figure 9: Tearing mode amplitudes through sawtooth.** The $m = 1$ modes do not correlate to electron temperature fluctuations near the sawtooth, when the $m = 0, n = 1$ mode is much larger than the $m = 1$ modes. This motivates the investigation into the effect of the $m = 0$ mode on the electron temperature during the sawtooth event.

of the mode growth during sawtooth events in 400 kA standard plasmas.

## 2.2 $m = 0$ Magnetic Mode Measurements and Calculations

Recent magnetic probe measurements and pseudospectral analysis has determined the $m = 0, n = 1 - 4$ mode structures at the edge of the MST in standard low current plasmas [18]. The structure and temporal evolution of the $m = 0, n = 1$ reconnected magnetic island through the sawtooth cycle has been well characterized. Also, computer simulations have been performed with the 3D non-linear resistive MHD code DEBS [19] to calculate the radial $m = 0, n = 1$ eigenfunction, which characterizes the radial "reach" of the tearing mode.

The radial magnetic fields arising from tearing modes were calculated in both the horizontal and vertical directions, in both cylindrical and toroidal geometries. Most important to this thesis is the vertical field eigenfunction calculated in toroidal geometry, shown in figure 10. The $m = 0, n = 1$ mode, which is resonant at the plasma edge, does in fact reach into the core of the plasma and is finite on the plane sampled by the Thomson scattering diagnostic everywhere except at $R = R_0$ (or $r = 0$). Thus, we can expect some effect from the mode on the core electron temperature during sawtooth events when the mode amplitude is very large. This is in fact observed, and will be described in Section 4.

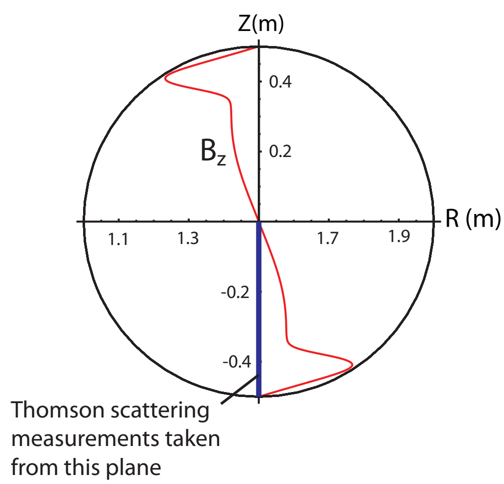


**Figure 10: Eigenfunction of dominant edge-resonant tearing mode (arb. units).** The vertical field eigenfunction is largest near the resonant surface of the $m = 0, n = 1$ mode, but remains finite until reaching the geometric center of the device. Thomson scattering measurements are taken on the lower vertical plane, which samples a finite $m = 0, n = 1$ eigenfunction for all minor radii except at $R = R_0$ (or $r = 0$). Graphic adapted from T. Tharp's Ph.D thesis [18].

Detailed measurements were taken of the edge magnetic field structure, allowing resolution of the $m = 0, n = 1$ magnetic island through sawtooth events. The temporal evolution of the magnetic flux through the sawtooth cycle is shown in figure 11. The horizontal axis is the toroidal angle of MST showing a full $2\pi$ radians, and the vertical axis is the depth into the plasma from the wall of the containment vessel. Prior to the sawtooth the mode is small with a very weak, localized reconnected island. During the sawtooth rise-phase, the island grows radially and strengthens as evidenced by the number of flux lines which form the island. After the sawtooth, magnetic energy has been removed from the plasma as seen by the reduction in the number of magnetic field lines, which is proportional to the magnetic energy. After the sawtooth the island quickly shrinks and the pre-sawtooth structure is observed with an overall reduction in magnetic flux due to magnetic energy being removed from the plasma. Also note that the center of the $m = 0, n = 1$ island shifts slightly outward through the sawtooth event.

These plots show that there is a well-defined $m = 0, n = 1$ magnetic island during sawtooth events, so we would expect some sort of temperature structure near the edge of the plasma with the same sort of structure. In the following sections we will correlate electron temperature measurements to the $m = 0, n = 1$ mode, and in fact an electron temperature island with the $m = 0, n = 1$ mode structure is observed.

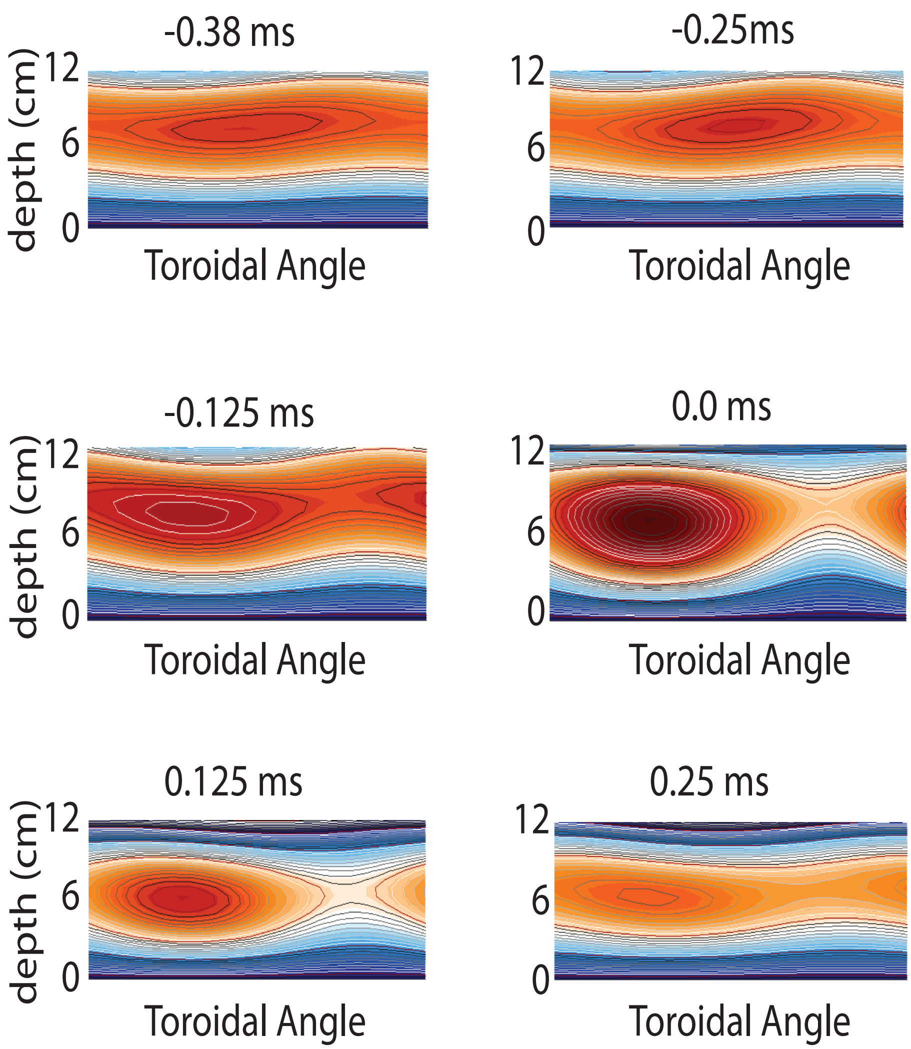


**Figure 11: Magnetic island evolution at edge of plasma.** As the sawtooth cycle progresses, the magnetic island grows radially and strengthens as more field lines reconnect. The island quickly dissipates to its pre-sawtooth size with an overall reduction in flux indicative of the magnetic energy lost during reconnection. Figures adapted from T. Tharp's Ph.D thesis [18].

# 3 Calculating $T_e$ Fluctuations

Calculation of electron temperature fluctuations involves a statistical technique called Bayesian analysis. During the analysis, a two-parameter model is fit to the measured electron temperature and a probability distribution is calculated for one of the parameters. Performing this analysis for many measured fluctuations (many laser pulse-bursts) results in 50 or more distribution functions for an ensemble of sawtooth events. The distribution functions are then multiplied together, giving a narrow distribution which determines the most-likely value and uncertainty of the parameter.

## 3.1 The Model

Bayesian statistics finds the most-probable value of a quantity given measured data and a theoretical model. Because the Thomson scattering diagnostic collects data at 25 kHz but tearing modes rotate at about 20 kHz, the Nyquist sampling theorem [20] is not satisfied. (The data collection rate is not greater than twice the frequency of the measured quantity.) Because of this limitation the total electron temperature fluctuation near the frequency of tearing modes cannot be determined with only Thomson scattering data. More information must be put into the temperature fluctuation model. By assuming that the electron temperature fluctuates in phase with a magnetic tearing mode, information about the phase of the mode can be added to the model. Such a model takes advantage of the high spatial resolution of Thomson scattering and the high temporal resolution of magnetic field pick-up coils.

The chosen model contains a fluctuating temperature amplitude and the phase of a magnetic tearing mode. It is given by,

$$T_e = T_{e0,m,n} + \tilde{T}_{e,m,n} \cos \Delta_{TS,m,n}. \tag{12}$$

Again, $T_e$ is the model electron temperature, $T_{e0,m,n}$ is a mean or background component, and $\tilde{T}_{e,m,n}$ is the fluctuating component of the electron temperature in phase with the magnetic mode adjusted to the Thomson scattering location, $\Delta_{TS,m,n}$. After the analysis, the full model can then be plotted as a function of toroidal angle as

$$T_e = T_{e0,m,n} + \tilde{T}_{e,m,n} \cos \phi_{m,n}. \tag{13}$$

The toroidal and poloidal mode numbers must still be factored into the equation because different $n$ numbers yield different types of toroidal structures for $m = 0$ modes. For the remainder of this thesis, the $(m, n)$ subscripts on electron temperature symbols will be clear from context and may be omitted.

The definition of the phase $\Delta_{TS,m,n}$ is complicated by the location of diagnostics on the MST vacuum chamber. The Thomson scattering diagnostic measures electron temperature at poloidal position $\theta_{TS} = -90°$ and toroidal position $\phi_{TS} = 222°$. Magnetic measurements are taken by the toroidal array (TA) of 64 magnetic field pick-up coils located within the MST vacuum vessel [9]. Phases are calculated relative to $\phi_{TA} = 0°$ and $\theta_{TA} = 241°$. Adjustments must also take into account the mode numbers of the magnetic fluctuation, $(m, n)$. The phase at the Thomson scattering position is [16, 17]

$$\Delta_{TS,m,n} = \Delta_{TA,m,n} + m(\theta_{TS} - \theta_{TA}) - n(\phi_{TS} - \phi_{TA}) \tag{14}$$

where $\Delta_{TA,m,n}$ is the phase of the $(m, n)$ magnetic mode calculated from Fourier analysis of magnetic coil data. The coils are poorly calibrated to resolve $m = 0$ modes, so an additional routine developed by J. Sarff was used to calculate the $m = 0$ mode phases. The routine re-calibrates the raw signals for each required measurement for only the time frame of interest, improving the accuracy of the measurement.

## 3.2 Determining the Fluctuation

Determining a fluctuation that has uncertainty is limited by a finite number of measurements. Figure 12 shows that more than one possible fluctuation has a finite probability of being true given the available data. Thus, for every measured fluctuation, an infinite number of models must be kept track of. Bayes' Theorem [21] provides a way to determine the probability that a particular model is true given available data.

Recall the notation for probability: $P(X|Y, I)$ is "the probability that the value $X$ is true given data $Y$ and background information $I$." Bayes' Theorem applied to Thomson scattering measurements is expressed as [16, 17]

$$P(\tilde{T}_e, T_{e0}|T_{e,1}, T_{e,2}, ..., T_{e,N}, I) \propto P(\tilde{T}_e, T_{e0}|I) \prod_i^N P(T_{e,i}|\tilde{T}_e, T_{e0}, I). \tag{15}$$

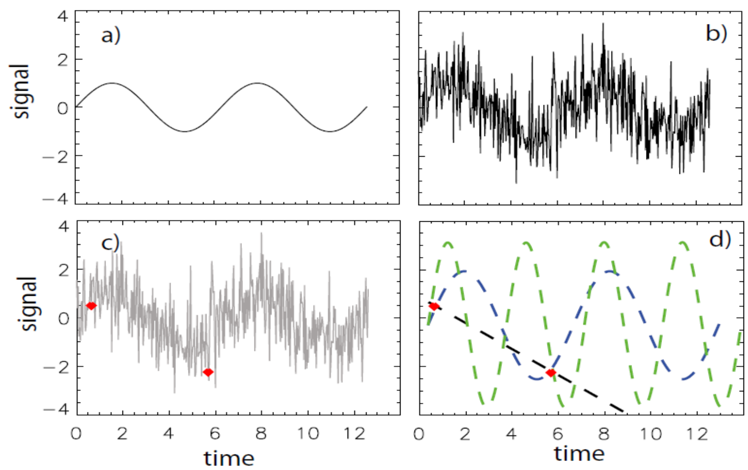


**Figure 12: Resolving a fluctuating signal.** a) Ideally, a fluctuating signal would have no uncertainty and could be measured continuously in time, giving the signal shown. b) In reality, all fluctuating signals will have a level of uncertainty. Shown here is a signal with uncertainty levels equal to the fluctuation amplitude. c) The two red points are hypothetical data collected by Thomson scattering. d) Many fluctuations can be fit to two data points, only one of which is the true fluctuation. Graphic courtesy of H. Stephens [16].

The left hand side represents the probability that a model characterized by two parameters $T_{e0}$ and $\tilde{T}_e$ is true. The measured data is $T_{e,i}$, where $i$ represents the laser pulses which resolve the fluctuation. $N$ can range from $2-6$. At least two measurements are needed to correlate and a maximum of six measurements resolve the fluctuation in a single Thomson scattering pulse-burst. The background information $I$ is the phase of the magnetic fluctuation.

The right hand side of equation 15 is Bayes' Theorem applied to the Thomson scattering measurements. The first function is the probability that the model is true given only the background information. The second function is a product of the probabilities for each laser pulse that the measured temperature is true given the model parameters and background data. This function represents the correlation of each electron temperature measurement within a fluctuation to the magnetic phase and to the other measurements for the given fluctuation.

Assuming a Gaussian probability distribution of the measured electron temperature, the right hand side can be calculated as [16, 17]

$$P(T_e|\tilde{T}_{e,m,n}, T_{e0}, I) = \frac{exp(-\frac{1}{2}\chi^2)}{\sigma\sqrt{2\pi}} \quad (16)$$

$$\chi^2 = \left(\frac{T_e - T_{e,model}(\tilde{T}_{e,m,n}, T_{e0}, \Delta_{TS})}{\sigma}\right)^2 \quad (17)$$

where the subscript $i$ has been dropped and it is assumed that the first term on the right hand side of equation 15, $P(\tilde{T}_e, T_{e0}|I)$, is flat for reasonable values of $T_{e0}$ and $\tilde{T}_e$. The quantity $\sigma$ is the error associated with the measured electron temperature, $T_e$, taken directly from stored Thomson scattering data.

Equations 15-17 now provide a probability distribution function for combinations of $\tilde{T}_e$ and $T_{e0}$. What is needed is a probability distribution for a single parameter so the fluctuating or background quantity can be determined separately. To find the probability distribution function for $\tilde{T}_e$, equation 15 is integrated over all realistic values of $T_{e0}$. The procedure is reversed to find the probability distribution for $T_{e0}$. The integration procedure is called statistical marginalization, where the marginalized parameter is the value being integrated over. Now a probability distribution function for a single parameter is known for each Thomson scattering pulse-burst.

The usefulness of Bayes' Theorem is that as more data is collected, the distribution functions found for each measured fluctuation can be multiplied together. With reasonably accurate assumptions and fluctuation models, the final probability distribution function will be fairly sharp. The ensemble thus greatly reduces the uncertainty in the measured fluctuation quantity. An example of collapsing distribution functions is shown in figure 13.

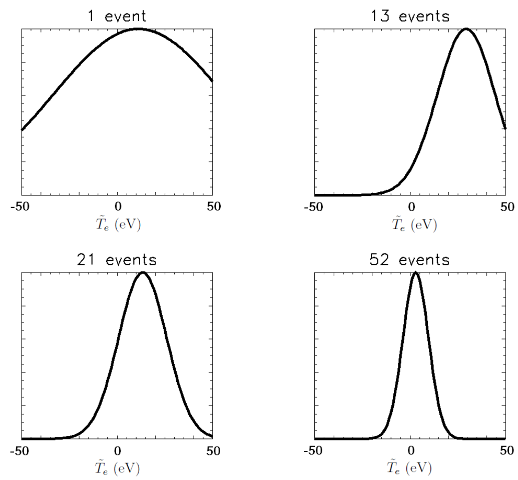


**Figure 13: Collapsing Bayesian distribution functions.** The final probability distribution function for $\tilde{T}_e$ is shown after multiplying different numbers of individual PDFs together. After one fluctuation measurement defined by a single burst of laser pulses the distribution is very wide. As more individual PDFs are multiplied the final PDF collapses, reducing the error in the analysis.

Once the final probability distribution functions for $\tilde{T}_e$ and $T_{e0}$ are found for an ensemble of data, the model quantities are taken to be the values at which the functions peak. The associated errors in the measurement are the locations at which the distributions fall off to $1/e$ of their peak value. Figure 14 is the result of the analysis for a single radial location for a 200 $\mu$s wide time range through the sawtooth cycle. The vertical dashed line is the most-probable electron temperature fluctuation and the two vertical red lines are the low and high error estimates.

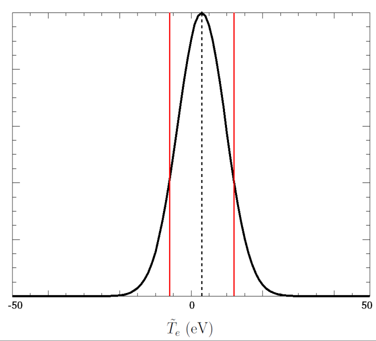


**Figure 14: Final Bayesian distribution function.** The result of Bayesian analysis is a single distribution function. The temperature fluctuation is given by the peak of the distribution (dashed line) with uncertainty given by the points where the distribution drops off to $1/e$ of the peak value (red lines). This particular measurement is interpreted as $\tilde{T}_e = 3$ eV with an upper error of 12 eV and lower error $-6$ eV.

# 4 Fluctuations Through Sawtooth Events

The fluctuation analysis was performed for Thomson scattering data taken in 400 kA standard MST plasmas and in 200 kA improved confinement plasmas. In order to ensure that every plasma discharge is similar enough to include in the data ensemble, several limits were placed on certain plasma parameters. Additionally, the magnetic mode is required to be rotating in order to resolve a fluctuation with a stationary diagnostic. The mode amplitudes must also be large enough for the mode to be considered real. These limits are summarized in table 1.

| Plasma parameter | Units | Lower bound | Upper bound |
|---|---|---|---|
| Current, $I_p$ | kA | 385 | 420 |
| Electron density, $n_e$ | $10^{13}$ cm$^{-3}$ | 0.85 | 1.15 |
| Mode phase velocity, $v_\phi$ | km/s | 2 | - |
| Mode amplitude, $\lvert b_t \rvert$ | G | 2 | - |

**Table 1: Parameter bounds used for fluctuation analysis in 400 kA standard plasmas.**

Electron temperature measurements were correlated to the $m = 0, n = 1$ magnetic tearing mode through the sawtooth cycle. The ensemble-averaged mode amplitude is shown in figure 15. The mode amplitude stays fairly small until about 0.2 ms before the sawtooth crash when it experiences rapid non-linear growth. After the crash the mode decays away more slowly.

Fluctuations were computed using the Bayesian analysis method developed in Section 3. To conduct the analysis, temperature measurements were grouped into 200 $\mu$s wide bins, with the $-400$ to $-200$ $\mu$s bin corresponding to $t = -0.3$ ms, etc. Smaller time windows were attempted, but the uncertainty associated with the

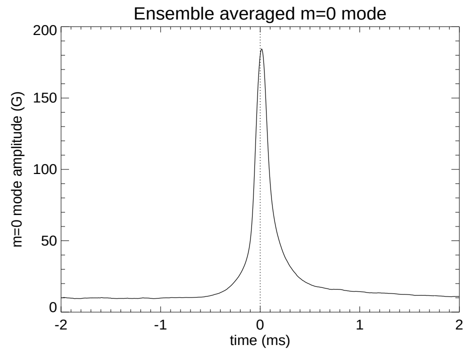


**Figure 15: Ensemble-averaged $m = 0, n = 1$ mode amplitude used in fluctuation analysis.** The mode amplitude is small before and after the sawtooth event, but experiences rapid non-linear mode growth beginning about 0.2 ms before the sawtooth crash.

fluctuation amplitudes was too high to draw any conclusions. Using 200 $\mu$s wide bins maximizes the amount of data available for the ensemble since a single burst of six Thomson scattering laser pulses occurs in exactly 200 $\mu$s. In principle wider time bins could be used to increase the likelihood of more Thomson scattering pulses falling in the time window, but this is not done for the reason outlined below.

Using such wide time bins limits the ability to resolve the fluctuation due to the rapid variation in the amplitude of the magnetic mode. Figure 16 is a plot of the $m = 0, n = 1$ mode amplitude through the sawtooth event. Overlaid on the plot are vertical lines which represent the edges of time bins. The mode amplitude changes significantly in 200 $\mu$s. For example, the +0.1 ms fluctuation measurement samples temperature fluctuations occurring at 0.0 ms, when the magnetic mode amplitude is near its peak, and at 0.2 ms, when the mode amplitude has decayed to less than $1/e$ of its maximum value. Thus, the measurement labeled 0.1 ms samples the effects of a wide range of mode amplitudes on the electron temperature. Using smaller time bins would in principle reduce this error, but fewer pulses in the smaller bin turns out to have a more adverse affect on the uncertainty of the measured fluctuation. 200 $\mu$s bins are exclusively used.

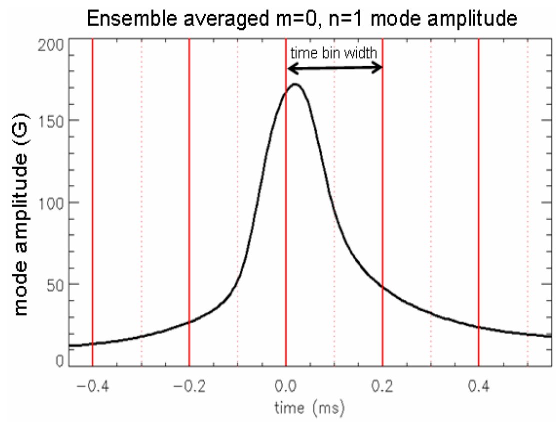


**Figure 16: Time bins used for fluctuation analysis.** 200 $\mu$s wide time bins sample a wide range of $m = 0, n = 1$ mode amplitudes.

The overall time window of interest is $-300$ $\mu$s to $+300$ $\mu$s which is split into 200 $\mu$s wide bins. The bins overlap which effectively "smooths" the data by using some measurements in multiple time bins. The phrase "prior to the sawtooth" refers to the time range from $-300$ $\mu$s to $-50$ $\mu$s. "During the sawtooth" refers to the brief period when the mode is largest, from 0.0 $\mu$s to approximately $+150$ $\mu$s, and "after the sawtooth" refers to the time range occurring after $+150$ $\mu$s. "Away from the sawtooth" refers to times far away from the time window of interest.

## 4.1 Fluctuations at the Edge

By drawing analogy to the work presented in Section 2, we can imagine two possible toroidal electron temperature structures associated with the $m = 0, n = 1$ magnetic mode. These two possible structures are illustrated in figures 17 and 18.

Figure 17 is a representation of an edge-localized electron temperature peak associated with the $m = 0, n = 1$ magnetic mode. The plot is a toroidal cross-section of the MST and shows a peak in the electron temperature profile, shown as color contours, with a structure similar to that of the $m = 0, n = 1$ magnetic island seen during sawtooth events. This structure should be localized near the resonant surface of the mode, which for $m = 0$ modes occurs near the plasma edge. This type of structure is referred to as a "heat-confining island" and is a direct analogy to the observed $m = 1, n = 5$ temperature structure.

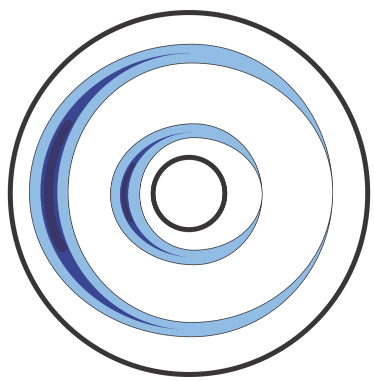

**Figure 17: Peaked toroidal electron temperature structure.** In analogy with previous results for $m = 1$ modes, we can expect a toroidal electron temperature structure associated with $m = 0, n = 1$ fluctuations which exhibits an edge-localized peaking, forming a heat-confining island.

Figure 18 is a representation of an isothermal electron temperature island forming with the same structure as the expected $m = 0, n = 1$ magnetic island. The plot is a toroidal cross-section of the MST and shows a flattening of the electron temperature profile near the edge represented by the color contour. This type of electron temperature profile is referred to as an "isothermal island" and is a direct analogy to the observed $m = 1, n = 6$ temperature structure.

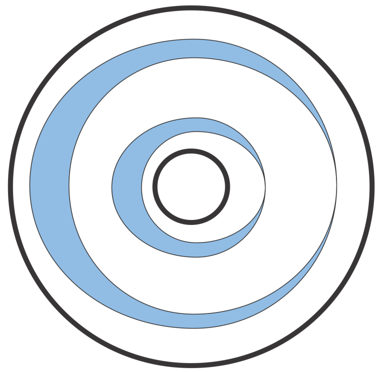

**Figure 18: Isothermal toroidal electron temperature structure.** In analogy with previous results for $m = 1$ modes, we can expect a toroidal electron temperature structure associated with $m = 0, n = 1$ fluctuations which exhibits an edge-localized flattening, forming an isothermal island.

#### 4.1.1 Observed electron temperature structures

Both types of edge structures are observed. Figure 19 is a plot of the electron temperature fluctuation amplitudes before and after the sawtooth. The upper plot is the fluctuation amplitudes just prior to the sawtooth event at $-0.05$ ms and the lower plot is the fluctuation amplitudes during the sawtooth at $+0.1$ ms.[2] The regions of interest are highlighted in gray. Notice that prior to the sawtooth there is a positive amplitude in the fluctuations at the edge but during the sawtooth there is a negative fluctuation amplitude at the edge. The behavior prior to the sawtooth is distinctly different than during the sawtooth.

The full electron temperature, $T_e = T_{e0} + \tilde{T}_e \cos\phi$, prior to the sawtooth is plotted at the edge at $\phi = 0$ and $\pi$ in figure 20. Highlighted in the gray area is the region

[2] Complete results for $m = 0, n = 1$ correlated fluctuations in 400 kA standard plasmas are presented in Appendix B.

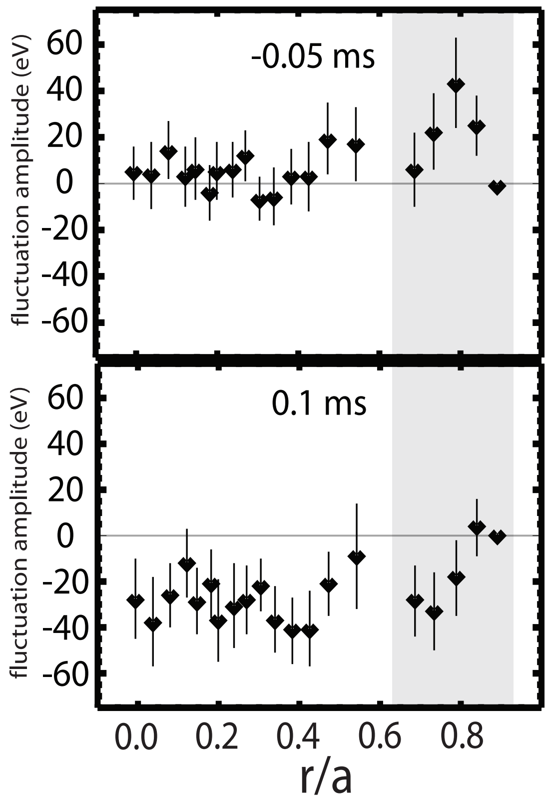


**Figure 19: Electron temperature fluctuation amplitudes through the sawtooth.** Near the edge there is a positive peak in the electron temperature fluctuation amplitude prior to the sawtooth and a negative trend during the sawtooth. During the sawtooth there is also a finite core fluctuation.

where the edge fluctuation is observed. At $\pi$ radians the electron temperature profile is linear and sharp, but at 0 radians the gradient region is higher and not as linear, suggesting that additional heat is being stored. This is indicative of a heat-confining island similar to the type of profile shown in figure 17. Figure 21 is a 2D color contour plot of the electron temperature at $-0.05$ ms. The horizontal axis covers the toroidal direction in the MST from $-\pi$ to $\pi$, and the vertical axis is the minor radius from the mid-radius to the edge. The color represents the full electron temperature in the region, with red being hot ($\approx$ 250 eV) and blue/purple being cold ($\approx$ 10 eV). The location of the heat-confining island is circled.

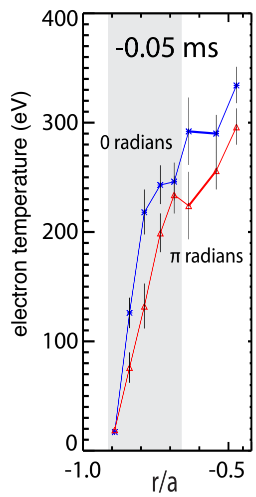


**Figure 20: Electron temperature profile near the edge prior to the sawtooth.** At $\phi = 0$ the electron temperature at the edge is hotter due to the $m = 0, n = 1$ correlated fluctuation than it is at $\phi = \pi$. This is indicative of a heat-confining island.

The full electron temperature during the sawtooth is plotted at $\phi = 0$ and $\pi$ in figure 22. The behavior at the edge is significantly different than before the sawtooth. At $\phi = \pi$ the edge gradient is still linear and sharp, but now at 0 radians a portion of the edge gradient is removed. This suggests that an isothermal island forms as shown in figure 18.

It is important to note that the radial resolution of the diagnostic near the plasma edge for the data used in this analysis is far from ideal. While the Thomson scattering system does have the capability to measure temperatures in this region with higher resolution, the dataset used in this analysis was intended to resolve core $m = 1$

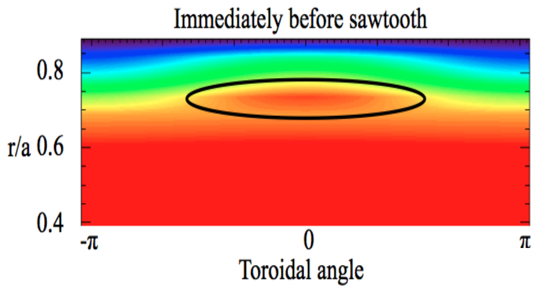


**Figure 21: 2D electron temperature near the edge prior to the sawtooth.** The heat-confining island is circled. The hottest point of the island is in the center and the temperature drops off near the edges, clearly depicting a heat-confining island.

correlated fluctuations as in references [16] and [17]. Thus the locations of the fiber optic light collection cables were chosen to maximize the radial resolution in the core of the MST and the edge was left poorly resolved. However, we do still observe an effect on the electron temperature due to correlated fluctuations, and thus we will proceed with the analysis.

#### 4.1.2 Relationship to magnetic structure

Previously the locations of the $m = 1, n = 6 - 7$ resonant surfaces were determined from the locations of the zero-crossings in the $\tilde{T}_{e,1,6-7}$ amplitudes (see Section 2). In the case of $m = 0, n = 1$ correlated temperature fluctuations there is no such zero-crossing. Therefore the radial location of the $m = 0$ resonant surface is estimated by finding the center of the heat-confining electron temperature island of figure 20. This location is at $r/a \approx 0.73$. During the sawtooth there is no clear island location so the resonant surface location cannot be estimated.

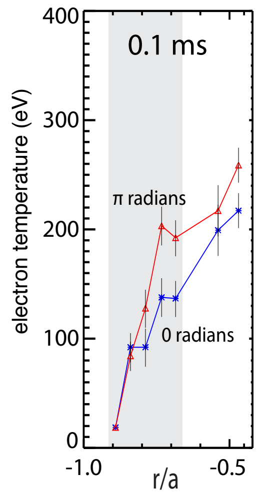


**Figure 22: Electron temperature profile near the edge during the sawtooth.** At $\phi = 0$ the electron temperature profile near the edge is flattened due to the $m = 0, n = 1$ correlated fluctuation, and at $\phi = \pi$ the temperature profile is sharp. This is indicative of an isothermal island.

Figure 23 shows the location of the $m = 0, n = 1$ (blue) and $m = 1, n = 6-7$ (red) resonant surfaces as measured by fluctuation analysis of Thomson scattering data plotted with the reconstructed q-profile (dashed line). As with the $m = 1$ modes, the location of the $m = 0, n = 1$ resonant surface measured by electron temperature fluctuations is well inside of the location predicted by the reconstructed q-profile.

The electron temperature islands are expected to exhibit the same toroidal structure as the $m = 0, n = 1$ magnetic island. The magnetic island has the structure depicted in figure 24. The "O-point" is defined as the widest part of the island and the "X-point" is the point where the island structure collapses, as labeled in the figure. Note that the magnetic field strength is represented by the density of field lines. By examining the density of the field lines at the O- and X-points in figures 11

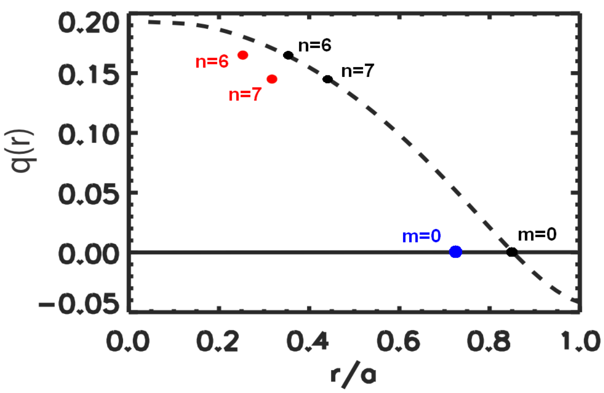


**Figure 23: Reconstructed q-profile with $T_e$ fluctuation-measured $m = 0, n = 1$ resonant surface location.** The blue point is the location of the $m = 0, n = 1$ resonant surface as measured by electron temperature fluctuation analysis and the red points are the locations of the $m = 1, n = 6 - 7$ resonant surfaces measured by electron temperature fluctuations. The black points are the locations of the resonant surfaces given by the reconstructed q-profile (dashed line). Figure adapted from H. Stephens' Ph.D thesis [16].

and 24, the field is clearly stronger at the O-point and weaker at the X-point. This information is important to determine the phase of the O- and X-points relative to Thomson scattering measurements.

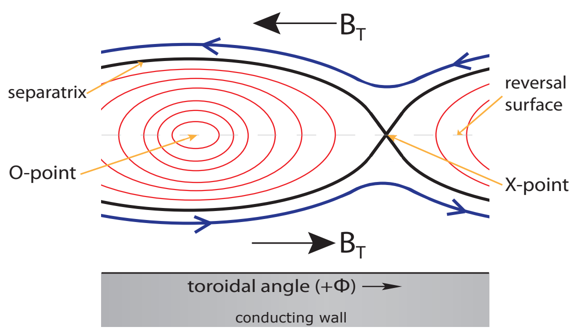


**Figure 24: Magnetic mode structure and sign conventions.** The field is stronger at the O-point and weaker at the X-point as seen by the field line density.

Magnetic modes are measured by a toroidal array of pick-up coils located at the wall outside the reversal surface and are stored as $\tilde{B}_{t,0,n} = |b_{t,0,n}| \cos{(n\phi - \Delta_{TA,0,n})}$. For the data used in the temperature fluctuation analysis the equilibrium toroidal field at the wall, $B_{t,wall}$, was conventionally positive.[3] Thus the O-point of the $m = 0, n = 1$ magnetic island is at the toroidal phase corresponding to a maximum $B_{t,wall} + \tilde{B}_{t,0,1}$. This maximum is achieved when

$$\phi - \Delta_{TA,0,1} = 0. \tag{18}$$

The X-point of the mode is at the toroidal phase corresponding to a minimum $B_{t,wall} + \tilde{B}_{t,0,1}$. This condition is met when

$$\phi - \Delta_{TA,0,1} = \pi. \tag{19}$$

The phase of the electron temperature fluctuations relative to the O- and X-points of the magnetic mode are found from the location of the Thomson scattering diagnostic, $\phi_{TS}$, and from equations 14 and 18. The phase at the toroidal array when the O-point is at the Thomson scattering diagnostic is $\Delta_{TA,0,1} = \phi_{TS}$. Plugging this into equation 14 yields the condition that $\Delta_{TS,0,1} = 0$ at the O-point. This is in agreement with the observed electron temperature structures. The heat-confining island prior to the sawtooth and the isothermal island during the sawtooth are both widest at $\phi = \Delta_{TS,0,1} = 0$. Repeating the analysis for the X-point yields the condition that $\Delta_{TS,0,1} = -\pi = \pi$, where the negative sign is unimportant because cosine is an

[3] This is in contrast to standard MST magnetic mode analysis which uses the convention that the average toroidal field, $B_{t,ave}$, is positive (making $B_{t,wall}$ negative in reversed-field discharges).

even function. Again this agrees with electron temperature fluctuation measurements which show no structure at the edge at $\pi$ radians.

## 4.2 Fluctuations in the Core

During the sawtooth event from 0.0 ms to 0.15 ms there is a finite core electron temperature fluctuation associated with the edge-resonant $m = 0, n = 1$ magnetic mode. The lower plot in figure 19 shows a clear electron temperature fluctuation across the entire minor radius of the plasma at +0.05 ms.[4] All core electron temperature fluctuations are non-zero within uncertainty indicating that the edge-resonant $m = 0, n = 1$ magnetic mode affects the core electron temperature.

Another interesting observation is a slight radial variation in the core electron temperature fluctuation amplitudes with radius for a given time point. Figure 25 is a plot of the fluctuation amplitudes for only the core of the plasma at +0.1 ms. Overlaid on the plot is a sinusoidal curve which approximates the variation seen in the fluctuation amplitudes with radius. The amplitude of the radial variation is about 10 eV and the wavelength is roughly 10 cm. This type of radial variation appears at each time point where a core electron temperature fluctuation is observed. More data is required to lower the uncertainty in the fluctuation amplitudes and characterize the radial variation.

The core electron temperature fluctuation has a dramatic effect on the overall electron temperature profile. Due to the toroidal nature of the $m = 0, n = 1$ mode, visualizing the effect on the profile requires 2D color contour plots. Reproducing

[4]The core fluctuations at other times during the sawtooth can be found in Appendix B

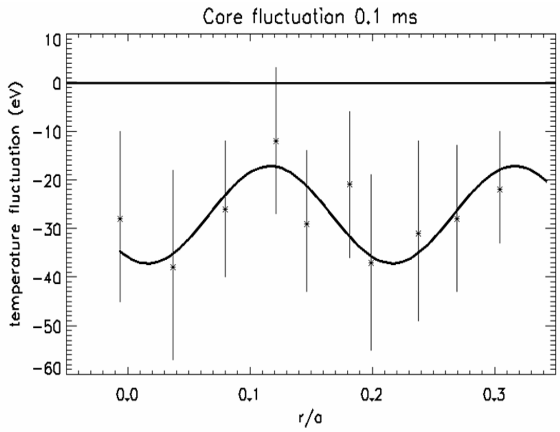


**Figure 25: Radial core $\tilde{T}_e$ variation during sawtooth crash.** The core electron temperature fluctuations exhibit a sinusoidal radial variation for all time points where a core fluctuation is observed. The amplitude of the variation is about 10 eV and the wavelength is about 10 cm.

many of these plots on paper is not feasible, but figure 26 shows a single plot of the overall electron temperature profile at 0.0 ms. The horizontal direction represents the toroidal angle $\phi$ and ranges from $-\pi$ to $+\pi$. The vertical axis is the normalized minor radial coordinate $r/a$, ranging from $-0.006$ to $+0.90$, covering the full radial range of the Thomson scattering data collected in this dataset.

Clearly visible in the color contour plot of the electron temperature is a hot/cold region in the core that depends on toroidal angle. The radial structure of the electron temperature is also clearly visible. This plot is illustrative of the effect of the $m = 0, n = 1$ mode on the electron temperature in that it clearly shows that the edge-resonant mode is reaching into the core and affecting the temperature there. The toroidally varying edge fluctuation is also clearly visible.

Initially the presence of a *core* electron temperature fluctuation correlated to the *edge-resonant* $m = 0, n = 1$ tearing mode seems surprising. However, there are two

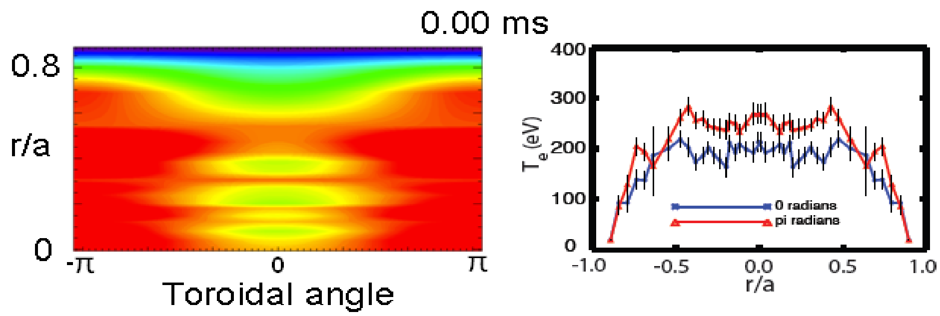


**Figure 26: Color contour plot showing $T_e$ profile at sawtooth crash.** The horozontal axis represents the toroidal angle ranging from $-\pi$ to $+\pi$, the vertical axis is the normalized minor radial coordinate, $r/a$, ranging from $-0.006$ to $+0.9$, and the color represents $T_e$, with red being hot ($\approx 250$ eV) and blue/purple cold ($\approx 10$ eV). The core electron temperature fluctuation creates a hot/cold variation in the core of the plasma. The radial structure of the fluctuation is also clearly visible.

possible explanations for the observed fluctuation. The first is that the radial extent of the $m = 0, n = 1$ mode as characterized by its eigenfunction (figure 10) does in fact reach into the core. The second explanation is more subtle. The finite $m = 1$ magnetic modes in the core of the plasma could be coupling together to give the radially-varying core fluctuation.

The $m = 0, n = 1$ mode eigenfunction clearly shows that the mode amplitude is in fact largest near the edge of the plasma. However, it remains finite through the entire plane sampled by the Thomson scattering diagnostic and only goes to zero at the geometric center of the device where $r/a = 0$. Thus, when the mode amplitude is extremely large, as it is in standard sawtooth events, we do expect the mode to have a significant radial reach into the core of the plasma.

From 0.0 to +0.15 ms there is a finite core electron temperature fluctuation observed across the entire minor radius of the plasma.[5] Figure 27 is a plot of the

[5]See figures in Appendix B.

$m = 0, n = 1$ and the $m = 1, n = 5-8$ mode amplitudes through the sawtooth cycle. The temperature fluctuations are largest at 0.0 ms when the $m = 0, n = 1$ mode is largest and gradually move toward zero as the $m = 0, n = 1$ mode decays. In this time region the $m = 1, n = 5-8$ modes are relatively large. By +0.2 ms the core electron temperature fluctuations have vanished to zero within uncertainty. At this time point the $m = 0, n = 1$ mode is leveling off at a small value and the $m = 1$ mode amplitudes have decayed considerably since +0.15 ms. Thus temperature fluctuations are only observed when both the $m = 0, n = 1$ and the core $m = 1$ modes are large, making it is possible that there is a connection between the $m = 0, n = 1$ correlated temperature fluctuations and the $m = 1, n = 5-8$ modes.

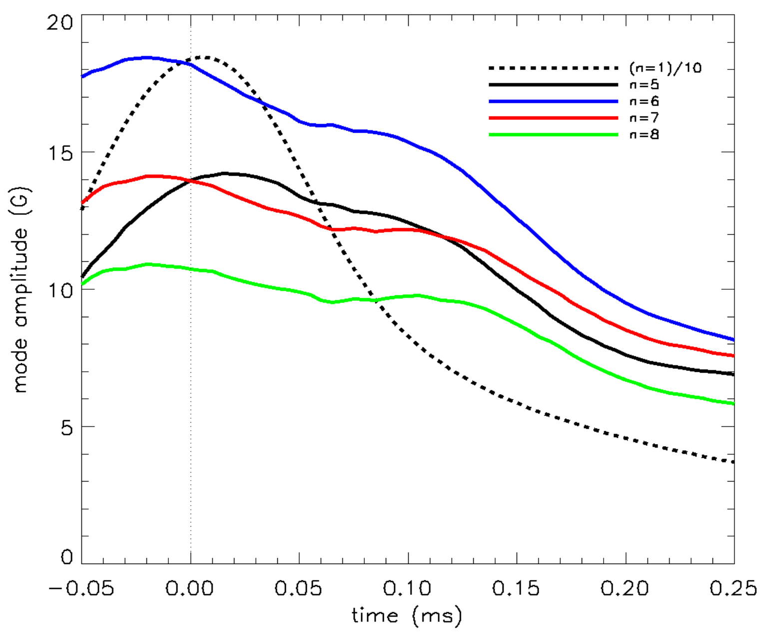


**Figure 27: The $m = 0$ and $m = 1$ mode amplitudes during sawtooth crash.** The core $m = 1$ magnetic modes are relatively large when the $m = 0, n = 1$ mode is largest and core electron temperature fluctuations are observed. When the $m = 0$ and $m = 1$ modes have decayed no core electron temperature fluctuations are observed.

The trend between the $m = 0$ and $m = 1$ mode amplitude evolution and the core electron temperature fluctuation evolution is by no means conclusive evidence that the $m = 1$ modes play a role in creating the core electron temperature fluctuation during the sawtooth. However the link between the modes and the electron temperature fluctuations described above does motivate additional study into the phenomena. A detailed analysis of three-wave coupling between $\tilde{T}_{e,0,1}$, $\tilde{T}_{e,1,n}$, and $\tilde{T}_{e,1,n+1}$ for $n \geq 5$ would help determine the true nature of the observed $m = 0, n = 1$ correlated electron temperature fluctuations. Such an analysis is beyond the scope of this thesis and may not be possible with the current Thomson scattering diagnostic and fluctuation analysis methods.

## 4.3 Connections to Ensemble-Averaged Temperature

A link can be made between $m = 0, n = 1$ correlated temperature fluctuations and the ensemble-averaged electron temperature evolution through the sawtooth cycle. J. Reusch has created a large ensemble of sawtooth events in 400 kA standard plasmas to study electron thermal transport [22]. A large number of electron temperature measurements allow binning at 20 kHz (50 $\mu$s) resolution without sacrificing the uncertainty of the measurements. The temporal behavior of the equilibrium electron temperature through the sawtooth cycle from this dataset is shown in figure 28. $T_e$ is the ensemble-averaged electron temperature taken directly from the Thomson scattering fitting routine with no additional processing.[6] Implicitly, $T_e$ is an average over all electron temperature fluctuations since the mode phases are randomly distributed

[6]Note that $T_e$ is not the same as $T_{e0}$ from the fluctuation analysis. $T_{e0}$ assumes a single fluctuation in phase with the $m = 0, n = 1$ magnetic tearing mode while $T_e$ is the ensemble-averaged electron temperature.

with respect to individual measurements in the ensemble. The ensemble-averaged core $T_e$ drops about 100 eV from 0.0 to +0.2 ms during the sawtooth.

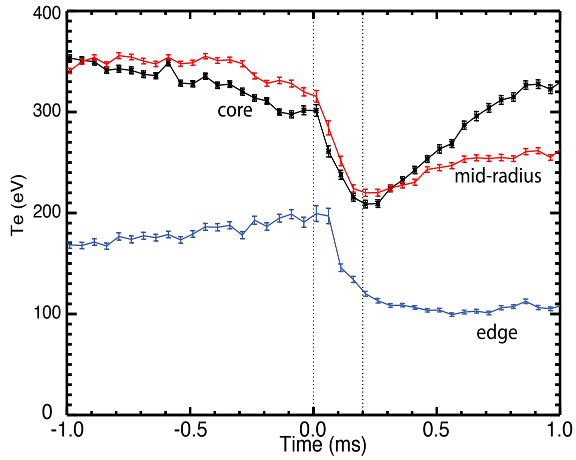


**Figure 28: Ensemble-averaged electron temperature evolution through the sawtooth.** In the core and mid-radius $T_e$ decreases fairly slowly until right at the sawtooth crash when it plummets by about 100 eV. At the edge the temperature rises until about 100 $\mu$s after the crash.

Figure 29 shows the core electron temperature from the fluctuation analysis at $\phi = 0$ and $\pi$ and also the ensemble-averaged core electron temperature for the time period of interest after the sawtooth. The core electron temperature at $\pi$ radians from 0.0 ms to +0.2 ms tracks well with the ensemble-averaged core electron temperature while the core temperature at 0 radians is much lower. At +0.2 ms, the correlated core electron temperatures at $\phi = 0$ and $\pi$ match each other and also match the ensemble-averaged core temperature. After +0.2 ms the correlated temperature fluctuations have vanished, leaving behind a much colder core.

It appears that at $\pi$ radians the core electron temperature from the fluctuation

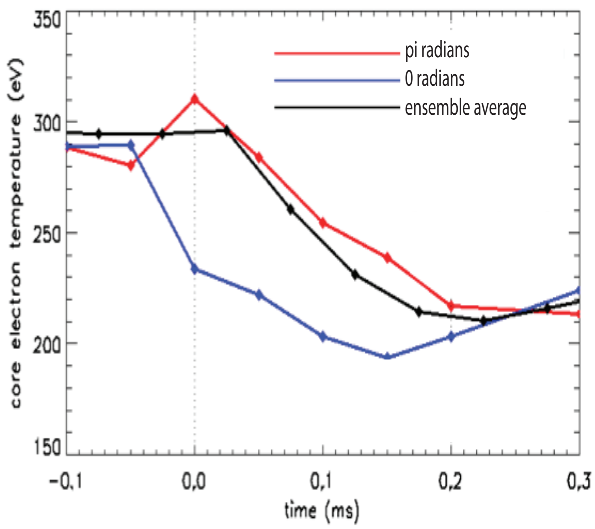


**Figure 29: Core electron temperature evolution through sawtooth.** At $\phi = \pi$ the core temperature matches the ensemble-averaged electron temperature while the temperature at $\phi = 0$ is much lower.

analysis is doing what the bulk plasma is doing (i.e. it approximately matches the ensemble-averaged electron temperature). However at 0 radians the core temperature differs from the ensemble average by a significant margin. Naively we would expect the core temperatures from the fluctuation analysis to bracket the ensemble-average (i.e. $T_e \approx T_{e0}$) but this is not observed. Instead the temperature at 0 radians is much colder, indicating that the $m = 0, n = 1$ magnetic mode has a drastic effect on the core electron temperature at 0 radians while leaving the temperature at $\pi$ radians largely unaffected.

Another way to look at the effect of the $m = 0, n = 1$ tearing mode on core confinement is to examine the edge electron temperature gradients formed by the fluctuations. While the gradient itself is an indicator of the level of confinement, a better measure is the gradient normalized to the core temperature [23]. A large normalized gradient indicates good confinement. Figure 30 is a plot of $\nabla_r T_{e,edge}/\bar{T}_{e,core}$ at $\phi = 0$ and $\pi$. The value of $\nabla_r T_{e,edge}$ is taken as the slope of the linear fit through the outermost five radial electron temperature measurements. This value is normalized to the average of the innermost 10 radial electron temperature measurements at either $\phi = 0$ or $\phi = \pi$,

$$\bar{T}_{e,core} = \frac{1}{10}\sum_{i=0}^{9}\Big(T_{e0}(r_i) + \tilde{T}_e(r_i)\cos\phi\Big), \tag{20}$$

where $r_i$ indicates the $i$-th radial measurement with $i = 0$ being the core-most location.

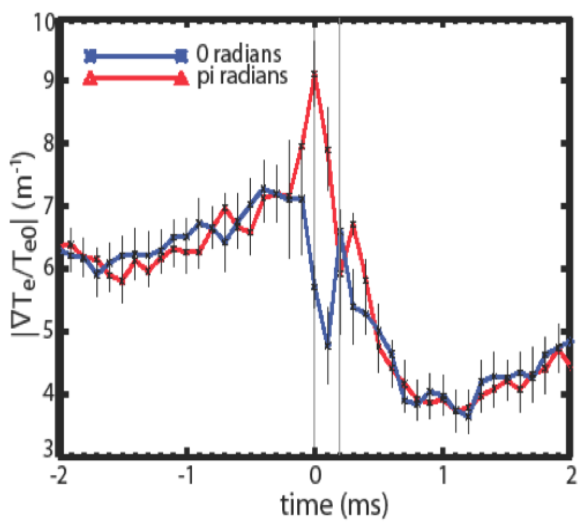


**Figure 30: Normalized edge electron temperature gradients.** Right after the sawtooth the gradient at $\phi = 0$ is much smaller, meaning that core confinement is poorer there than at $\pi$ radians.

At the sawtooth the normalized edge gradient at $\phi = 0$ is much lower than at $\phi = \pi$, suggesting that confinement is poorer at 0 radians. A lower edge electron temperature gradient allows heat to flow outward radially from the core so we expect the core temperature at $\phi = 0$ to be colder, consistent with figure 29. While we cannot determine what is causing the heat loss, it seems that the poor gradient at 0 radians arising from the $m = 0, n = 1$ correlated electron temperature fluctuation may be reducing core electron heat.

Naively, this data suggests that the $m = 0, n = 1$ magnetic mode "pokes a hole" in the core electron temperature at 0 radians while lowering the confining gradient at the edge. This allows the core temperature to cool rapidly at this location, giving the apparent $m = 0, n = 1$ core fluctuation. The core temperature everywhere else will respond to this rapid core heat loss at 0 radians, cooling in 200 $\mu$s. It appears that the $m = 0, n = 1$ tearing mode plays a role in determining core electron heat confinement during sawtooth events.

## 4.4 Correlations to the $m = 0, n = 2$ Magnetic Mode

Electron temperature fluctuations were also correlated to the $m = 0, n = 2$ magnetic mode which is resonant at the same location as the $m = 0, n = 1$ mode.[7] The plasma parameter bounds used for this analysis are the same as the $m = 0, n = 1$ correlations. Figure 31 shows a comparison between the ensemble-averaged $m = 0$ mode amplitudes through the sawtooth event. The $m = 0, n = 2$ amplitude is considerably smaller than the $m = 0, n = 1$ mode, so we would expect a weaker electron temperature correlation if there is any correlation at all.

Prior to the sawtooth there is no observed fluctuation within the uncertainty of the analysis. Figure 32 is a plot of the electron temperature fluctuation amplitudes prior to the sawtooth at $-0.05$ ms. All radial locations except a single point at

[7] Complete results for $m = 0, n = 2$ correlated fluctuations are presented in Appendix C

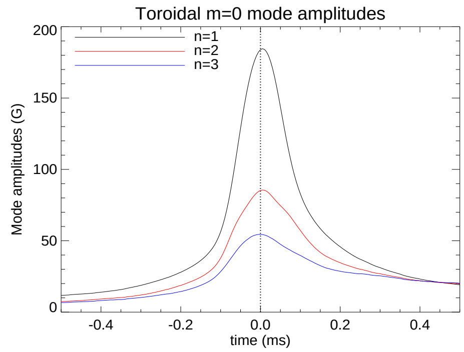


**Figure 31: Toroidal $m = 0, n = 1 - 3$ mode amplitudes through the sawtooth.** The $m = 0, n = 2$ mode amplitude is considerably smaller than the $m = 0, n = 1$, so we expect a smaller effect from the $m = 0, n = 2$ mode on electron temperature fluctuations.

$r/a \approx 0.3$ are zero within the uncertainty of the analysis. There are no correlated $m = 0, n = 2$ electron temperature fluctuations prior to the sawtooth in contrast with the $m = 0, n = 1$ mode.

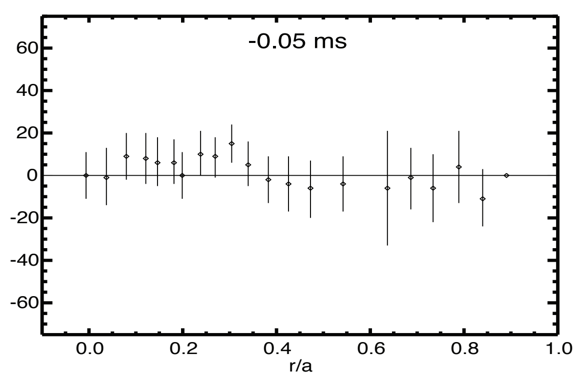


**Figure 32: $\tilde{T}_e$ amplitudes correlated to the $m = 0, n = 2$ mode prior to sawtooth.** There is only a single radial location with a finite fluctuation amplitude within the uncertainty of the measurement.

During the sawtooth, there is a general positive trend in the correlated temperature fluctuation amplitudes. It is unclear why the fluctuation amplitudes are positive when correlated to the $m = 0, n = 2$ mode and negative in the $m = 0, n = 1$ case. There is also a radial structure associated with the fluctuation. Figure 33 is a plot of the fluctuation amplitudes during the sawtooth at +0.10 ms. The fact that the core electron temperature fluctuation amplitudes are finite when correlated to the $m = 0, n = 2$ mode may mean that core $m = 1$ modes are playing a role as with the $m = 0, n = 1$ correlated fluctuations. Three-wave coupling analysis is needed to test the relationship between $m = 1$ modes and core temperature fluctuations.

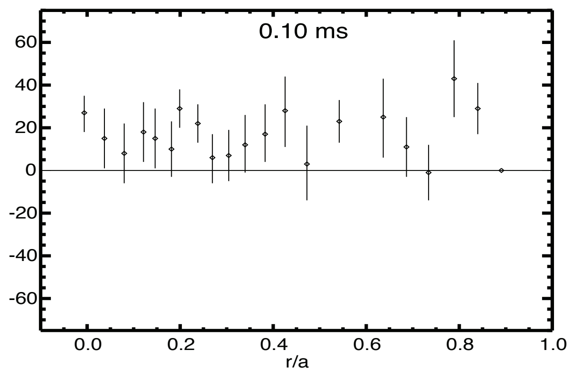


**Figure 33: $\tilde{T}_e$ amplitudes correlated to the $m = 0, n = 2$ mode during sawtooth.** There is a general positive trend in the fluctuation amplitudes with a radial structure.

The only conclusion we can make based on the $m = 0, n = 2$ correlated temperature fluctuations is that a single-fluctuation model is not sufficient to describe electron temperature fluctuations during the sawtooth. Both $n = 1$ and $n = 2$ correlated fluctuations are finite and occur in the same plasma volume, so a more accurate model must be developed which takes both effects into account simultaneously. Multi-parameter models are difficult with the Bayesian analysis techniques used in this thesis. The analysis reduces a two-parameter model ($T_{e0}$ and $\tilde{T}_e$) to single-parameter model using marginalization so the effect of variations in the marginalized parameter are removed. A new analysis technique would need to be employed to track the simultaneous effects of multiple parameters.

## 4.5 $T_e$ Fluctuations in Improved Confinement Plasmas

The fluctuation analysis was attempted in low current improved confinement plasmas where an inductive current control technique known as Pulsed Poloidal Current Drive (PPCD) [24] was employed. Plasma parameters used for the event ensemble are outlined in table 2. Note that the density bounds are much wider than those used for the 400 kA standard plasma event ensemble. Much less data was available in PPCD plasmas so wider bounds were necessary to increase the quantity of data available for Bayesian analysis.

| Plasma parameter | Units | Lower bound | Upper bound |
|---|---|---|---|
| Current, $I_p$ | kA | 150 | 225 |
| Electron density, $n_e$ | $10^{13}$ cm$^{-3}$ | 0.5 | 1.5 |
| Mode phase velocity, $v_\phi$ | km/s | 2 | - |
| Mode amplitude, $\lvert b_t \rvert$ | G | 2 | - |

**Table 2: Parameter bounds used for fluctuation analysis in 200 kA PPCD plasmas.**

Correlations to the $m = 0, n = 1$ mode were attempted but no quality results were obtained due to a number of factors. First, PPCD plasmas do not have true sawtooth events but instead have much smaller $m = 0$ mode activity termed "$m = 0$ bursts." The peak mode amplitudes for $m = 0$ bursts are on the order of 50 G, compared with 200 G for 400 kA standard plasmas. Second, there was only a small quantity of data available due to high levels of background light present in 200 kA PPCD plasmas. Background light limits the effectiveness of avalanche photodiode detectors which affects the quality of the final measured electron temperature. Each time bin through the sawtooth cycle had approximately 5 events per radial position in the Bayesian analysis routine, compared to more than 50 events per radial position for 400 kA standard plasmas. Bayesian analysis requires a large amount of data so the ability to resolve electron temperature fluctuations was severely limited.

Despite these limitations some fluctuations were still observed when the correlations were performed. Figure 34 shows plots of the electron temperature fluctuation amplitudes before and after the $m = 0$ burst. Important to note here is the change of scale of the vertical axes. The uncertainty of these fluctuations is extremely large and the fluctuations themselves can be very large. Prior to the $m = 0$ burst there is a possible fluctuation at the mid-radius of the plasma and nothing anywhere else. During the $m = 0$ burst it appears that the fluctuation has vanished. There is not enough data to say with confidence that a fluctuation exists. More data is needed to determine the effect of $m = 0$ bursts on electron temperature fluctuations in 200 kA PPCD plasmas.

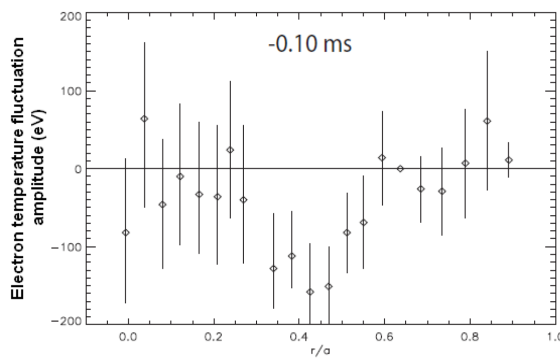


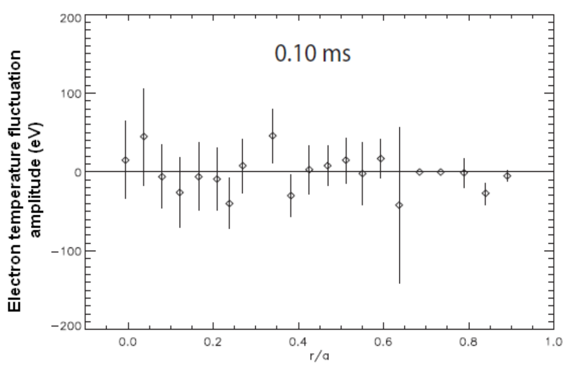


**Figure 34: $\tilde{T}_e$ amplitudes correlated to the $m = 0, n = 1$ mode during $m = 0$ bursts in PPCD plasmas.** The fluctuation amplitudes are much larger than in 400 kA standard plasmas with much larger uncertainties. Prior to the $m = 0$ burst there is a possible fluctuation at the mid-radius which then vanishes after the burst. No conclusions can be drawn from this analysis due to high uncertainty and limited data.

# 5 Summary

Electron temperature measurements taken with a 25 kHz multi-point, multi-pulse Thomson scattering diagnostic were correlated to the phase of the $m = 0, n = 1$ and $m = 0, n = 2$ tearing modes through sawtooth events in 400 kA standard RFP plasmas in the Madison Symmetric Torus. Measurements were also correlated to the phase of the $m = 0, n = 1$ mode in small "$m = 0$ bursts" in low current improved confinement plasmas.

## 5.1 Key Results

The most important result of the electron temperature correlations presented in this thesis is that the electron temperature in the core of the plasma correlates to edge-resonant $m = 0$ magnetic modes during sawtooth events in 400 kA standard RFP plasmas. This result is a bit surprising given the radial location of the $m = 0$ resonant surfaces, but after taking into account the mode's eigenfunction it is clear that when the $m = 0, n = 1$ mode amplitude is largest during the sawtooth crash, the eigenfunction in the core of the plasma can reach an appreciable value. This mode dominates the mode spectrum briefly during the sawtooth so it is not too surprising that electron temperature correlates to it in the core.

Prior to the sawtooth and near the edge of the plasma the correlated electron temperature fluctuation creates a heat-confining island which rotates toroidally around the MST. During the sawtooth the behavior of the island changes to isothermal. While the Thomson scattering diagnostic used to measure the temperature lacked high radial resolution in this region, an approximate location of the $m = 0, n = 1$ resonant surface was found by looking for the center of the observed structure. The resonant surface of the $m = 0, n = 1$ mode was found to be well inside of the predicted location from equilibrium reconstructions but in rough agreement with previous electron temperature correlation analysis.

Two possible explanations for the disagreement in the location of the $m = 0, n = 1$ resonant surface have been identified. The first is that the MSTFit code which produces the equilibrium reconstruction could fail to take some physics into account. This has not been further investigated. The second explanation is that the dataset used to determine electron temperature fluctuations most likely lacks sufficient edge resolution to accurately locate the $m = 0, n = 1$ resonant surface using Thomson scattering measurements. An additional discrepancy is that magnetic probe data (figure 11) and other measurements show that the resonant surface moves outward slightly during the sawtooth event but temperature fluctuation measurements cannot resolve any movement. With improved edge resolution and quality of Thomson scattering data the location of the $m = 0, n = 1$ island could be better determined for comparison to probe measurements.

Analysis of the data we do have suggests that the $m = 0, n = 1$ correlated electron temperature fluctuations have a large effect on core electron heat confinement during sawtooth events. The $m = 0, n = 1$ correlated core electron temperature profile at $\phi = \pi$ nearly matches the ensemble-averaged core electron temperature through the sawtooth while the electron temperature at 0 radians is much lower and has poorer confinement characteristics as evidenced by a smaller normalized edge gradient. This suggests that the $m = 0, n = 1$ tearing mode lowers the electron temperature by forming an isothermal temperature island at the edge at 0 radians. This allows heat to flow rapidly outward, thereby lowering the core electron temperature at 0 radians. The electron temperature in the core at other toroidal locations follows more slowly, resulting in an overall loss in core electron temperature through the sawtooth.

Another observation is that a radial structure appears within the core electron temperature fluctuation amplitudes, lasting as long as the core fluctuation. This radial perturbation could be the result of interactions between core $m = 1$ modes, but it is not well understood and has yet to be further investigated.

## 5.2 Future Work

Several things can be done to improve the results of the $m = 0$ correlated electron temperature fluctuations. The first and most important is to collect data with higher radial resolution at the edge region of the plasma. This is easily accomplished with the current Thomson scattering diagnostic by adjusting the viewing angle of several scattered light collecting fiber optic cables. In addition to adjusting the fibers, care needs to be taken to ensure that scattered light detectors are operating correctly and that the routine which finds the electron temperature from the measured data works properly.

The addition of the Fast Thomson scattering system currently being developed [25] will provide a dramatic increase in the quantity of data available for electron temperature correlations. This, combined with improved edge resolution, should provide a much clearer picture of the effect of the $m = 0, n = 1$ magnetic mode on the electron temperature during sawtooth events. Once a significant quantity of high-quality data is collected, the analysis done in this thesis should be performed again to confirm that the results are valid. The location of the $m = 0$ resonant surface should be found with a higher degree of confidence using temperature fluctuation data.

Once the results in this thesis are confirmed with more data, a multi-parameter model can be developed to evaluate the simultaneous effect of many magnetic modes. Of particular interest is the three-wave coupling interaction between $\tilde{T}_{e,0,1}$, $\tilde{T}_{e,1,6}$, and $\tilde{T}_{e,1,7}$. Determining the time and amplitude behavior of these fluctuations will give a clearer picture of why the $m = 0, n = 1$ mode affects the core electron temperature so dramatically during sawtooth events. Three-wave coupling analysis requires relative phase information between the fluctuating quantities which will be difficult to extract from Bayesian analysis, thus a new analysis technique will probably need to be developed.

Bringing in additional diagnostics can provide a measurement of core electron energy transport during sawtooth events. Cross-correlating electron density and temperature fluctuations may be possible using far-infrared polarimetry-interferometry measurements of the electron density. In the future electron density measurements may be available from Thomson scattering as well. Information about density fluctuations is needed to correlate with electron temperature fluctuations to calculate the electron energy transport.

# References

[1] J.D. Lawson. Some criteria for a power producing thermonuclear reactor. *Proc. Phys. Soc. B (UK)* **70**, A03620 (1957)

[2] Jeffrey P. Freidberg. *Plasma Physics and Fusion Energy*. Cambridge University Press, 2007

[3] Sergio Ortolani and Dalton D. Schnack. *Magnetohydrodynamics of Plasma Relaxation*. World Scientific, 1993

[4] J.B. Taylor. Relaxation of toroidal plasma and generation of reverse magnetic fields. *Phys. Rev. Lett.* **33**, 1139 (1974)

[5] J.D. Huba. *NRL Plasma Formulary*. Naval Research Laboratory, 2009

[6] B. E. Chapman, A. F. Almagri, M. Cekic, D. J. Den Hartog, S. C. Prager, and J. S. Sarff. Sawteeth and energy confinement in the Madison Symmetric Torus reversed-field pinch. *Phys. Plasmas* **3**, 709 (1996)

[7] Theodore M. Biewer. *Electron thermal transport in the Madison Symmetric Torus*. PhD thesis, University of Wisconsin - Madison, 2002

[8] R.N. Dexter, D.W. Kerst, T.W. Lovell, S.C. Prager, and J.C. Sprott. The Madison Symmetric Torus. *Fusion Technol* **19**, 131 (1991)

[9] D. Craig. Magnetic mode analysis in MST. MST internal document, May 2005

[10] J. A. Reusch, M. T. Borchardt, D. J. Den Hartog, A. F. Falkowski, D. J. Holly, R. O'Connell, and H. D. Stephens. Multipoint Thomson scattering diagnostic

for the Madison Symmetric Torus reversed-field pinch. *Rev. Sci. Instrum.* **79**, 10E733 (2008)

[11] Ian H. Hutchinson. *Principles of Plasma Diagnostics*. Cambridge University Press, 2002

[12] H. D. Stephens, M. T. Borchardt, D. J. Den Hartog, A. F. Falkowski, D. J. Holly, R. O'Connell, and J. A. Reusch. Calibration of a Thomson scattering diagnostic for fluctuation measurements. *Rev. Sci. Instrum.* **79**, 10E734 (2008)

[13] R. O'Connell, D. J. Den Hartog, M. T. Borchardt, D. J. Holly, J. A Reusch, and H. D. Stephens. Optimizing a Thomson scattering diagnostic for fast dynamics and high background. *Rev. Sci. Instrum.* **79**, 10E735 (2008)

[14] A.C. Selden. Simple analytic form of the relativistic Thomson scattering spectrum. *Phys. Lett. A* **79**, 405 (1980)

[15] D. J. Den Hartog, J. R. Ambuel, M. T. Borchardt, J. A. Reusch, P. E. Robl, and Y. M. Yang. Pulse-burst operation of standard Nd:YAG lasers. *J. Phys. Conf. Ser.* **227**, 012023 (2010)

[16] Hillary D. Stephens. *Electron Temperature Structures Associated With Magnetic Tearing Modes in the Madison Symmetric Torus*. PhD thesis, University of Wisconsin - Madison, 2010.

[17] H. D Stephens, D. J. Den Hartog, C. C. Hegna, and J. A. Reusch. Electron thermal transport within magnetic islands in the reversed-field pinch. *Phys. Plasmas* **17**, 056115 (2010)

[18] Timothy D. Tharp. *Measurements of Nonlinear Hall-Driven Reconnection in the Reversed Field Pinch*. PhD thesis, University of Wisconsin - Madison, 2010.

[19] D. D. Schnack, D. C. Barnes, Z. Mikic, Douglas S. Harned, and E. J. Caramana. Semi-implicit magnetohydrodynamic calculations. *J. Comput. Phys.* **70**, 330 (1987)

[20] H. Nyquist. Certain topics in telegraph transmission theory. *EIEE Trans.*, 617 (1928)

[21] D.S. Sivia. *Data analysis: a Bayesian tutorial*. Oxford University Press, 2006

[22] J. Reusch. Simulated and measured electron thermal transport with varying magnetic stochasticity in the MST RFP. *Bulletin of the American Physical Society* **55**, 104 (2010)

[23] A. Alfier, R. Pasqualotto, G. Spizzo, A. Canton, A. Fassina, and L. Frassinetti. Electron temperature profiles in RFX-mod. *Plasma Phys. Control. Fusion* **50**, 035013 (2008)

[24] J.S. Sarff, S.A. Hokin, H. Ji, S.C. Prager, and C.R. Sovinec. Fluctuation and transport reduction in a reversed field pinch by inductive poloidal current drive. *Phys. Rev. Lett.* **72**, 3670 (1994)

[25] W.S. Harris, D.J. Den Hartog, and N.C. Hurst. Initial operation of a pulse-burst laser system for high-repetition-rate Thomson scattering. *Rev. Sci. Instrum.* **81**, 10D505 (2010)

# A Toroidal Geometry and Coordinates

Toroidal geometry is best visualized by imagining a hollow cylinder bent until its two faces connect into a donut-like shape. Figure 35 shows toroidal geometry and coordinates.

Toroidal coordinates have elements of both cylindrical and spherical coordinates. The radial coordinate in cylindrical geometry, $r$, translates directly to toroidal geometry and is called the minor radial coordinate. Since the cylinder has been bent into another circle there is an additional radial coordinate called the major radius, given by $R$. Two angles are used as in spherical geometry but instead of "polar" and "azimuthal" they are termed "poloidal" and "toroidal." The poloidal angle, $\theta$, represents the angle swept out by the minor radius and the toroidal angle, $\phi$, represents the angle swept out by the major radius.

The toroidal and poloidal angles range from $-\pi$ to $\pi$ (or alternatively from 0 to $2\pi$). The minor radius ranges from 0 to $a$ and the major radius ranges from $R_0 - a$ to $R_0 + a$. In the Madison Symmetric Torus $R_0 = 1.5$ m and $a = 0.52$ m.

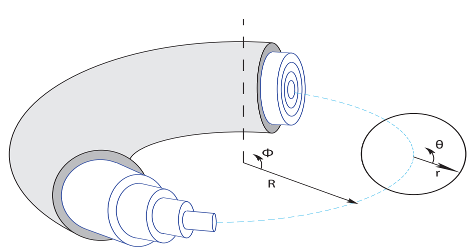


**Figure 35: Toroidal geometry and coordinates.** $R$ is the major radial coordinate, $r$ the minor radial coordinate, $\phi$ the toroidal angle, and $\theta$ the poloidal angle. Figure adapted from J. Sarff.

# B Complete $m = 0, n = 1$ Correlated Fluctuation Results

Below are the complete results of electron temperature fluctuations correlated to the $m = 0, n = 1$ magnetic mode during sawtooth events in 400 kA standard RFP plasmas. The left column are the fluctuations and the right column are the corresponding electron temperature profiles, $T_e = T_{e0} + \tilde{T}_{e,0,1} \cos\phi$, evaluated at $\phi = 0$ (blue) and $\phi = \pi$ (red). The time represents the time relative to the sawtooth event.

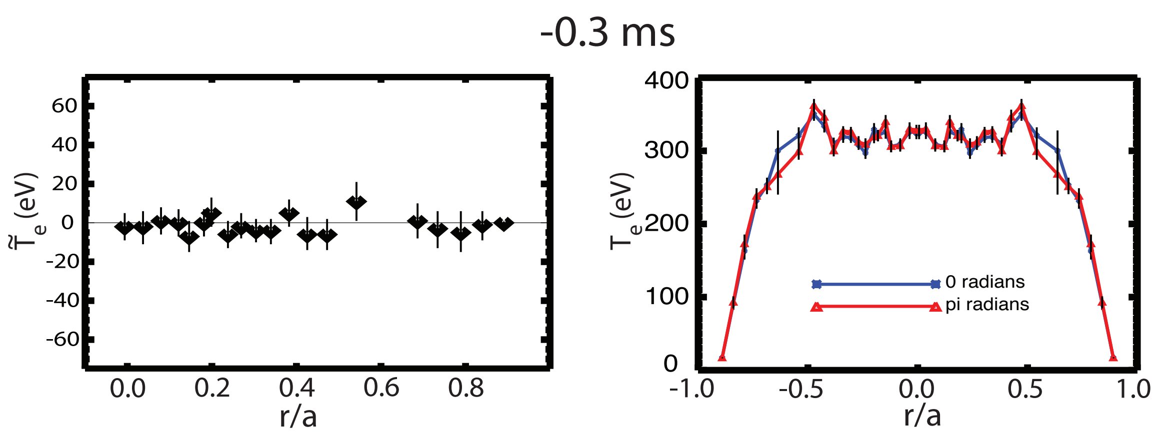

-0.2 ms

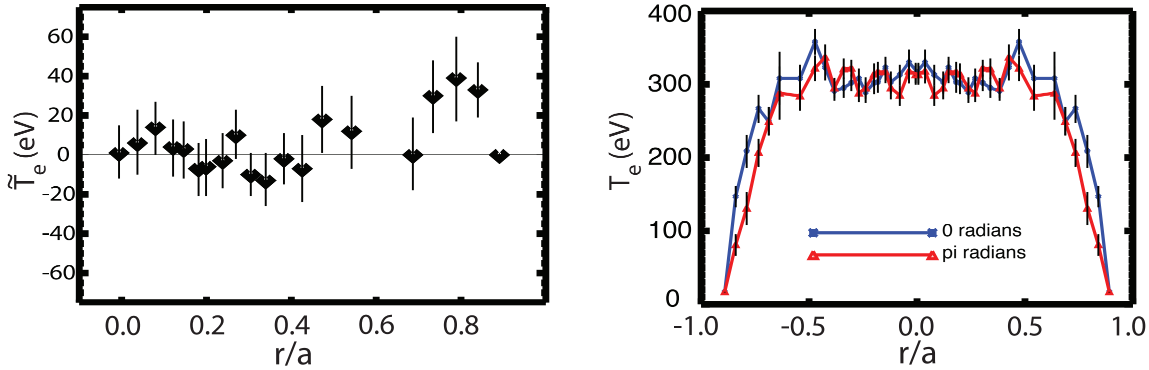


-0.1 ms

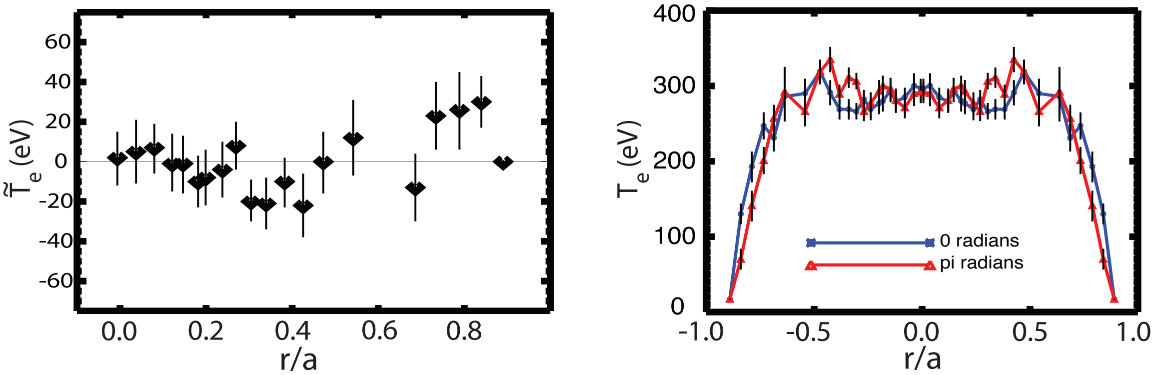


-0.05 ms

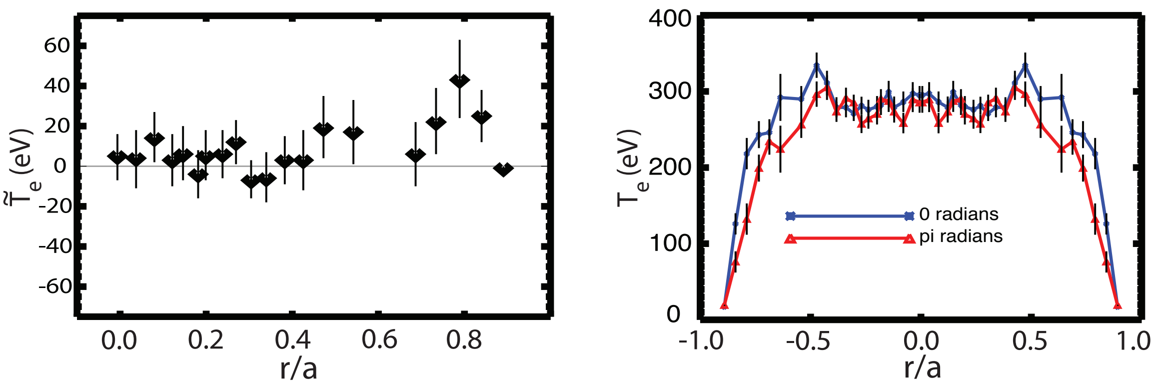

0.00 ms

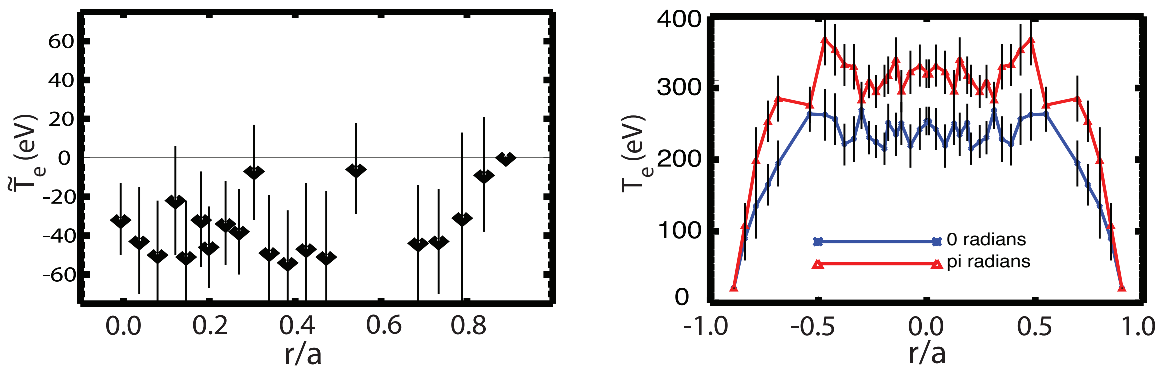


0.05 ms

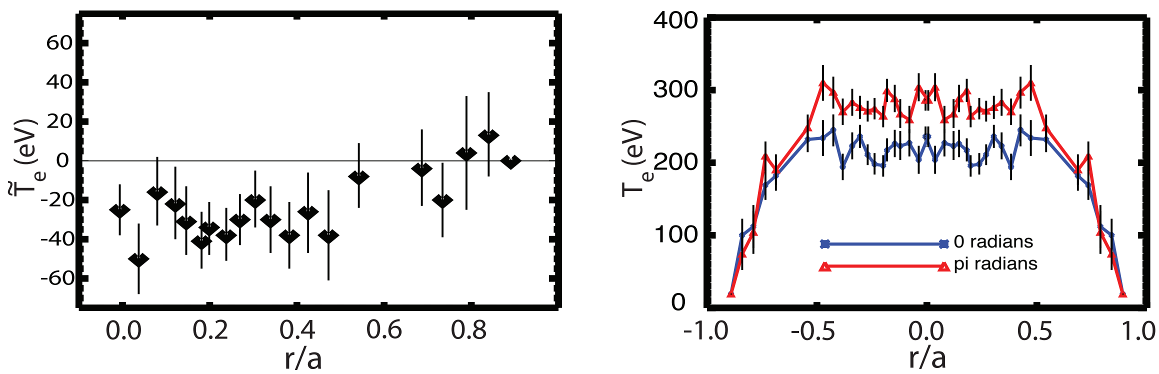


0.10 ms

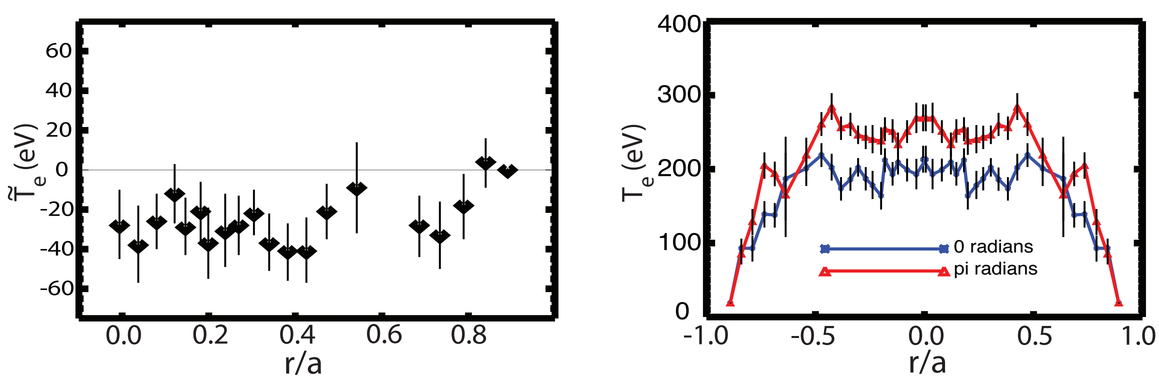

0.15 ms

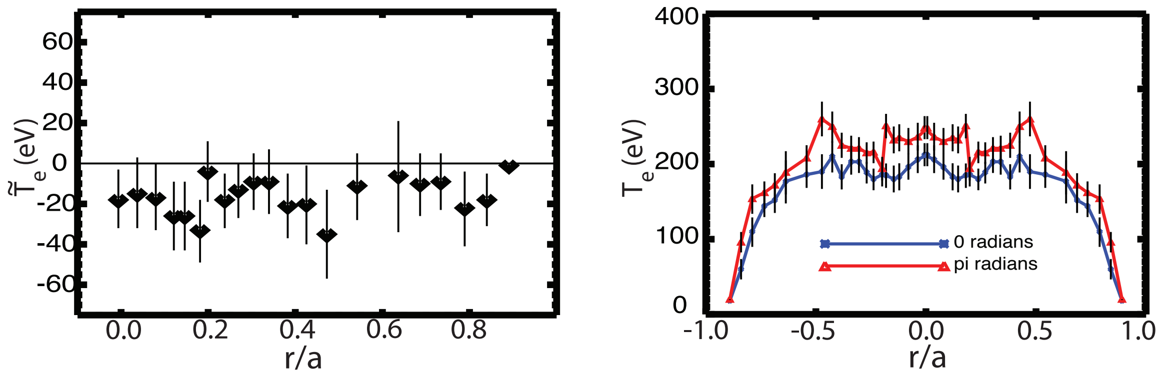


0.20 ms

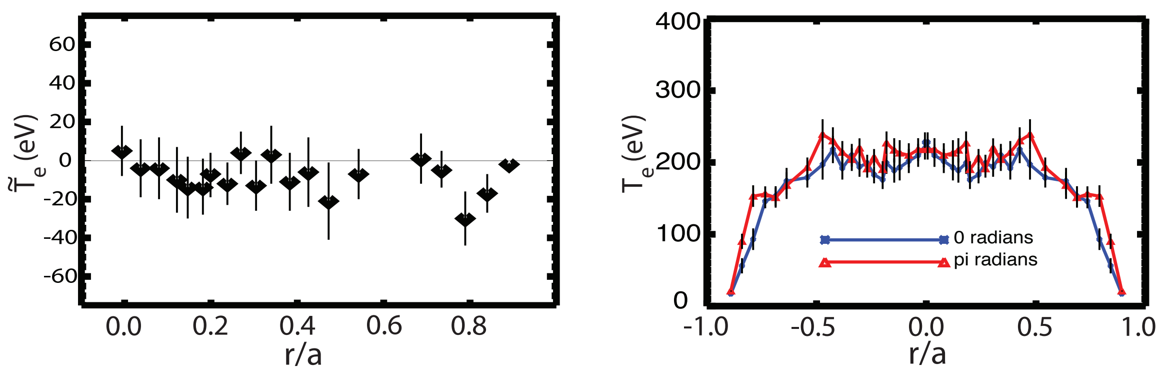


0.30 ms

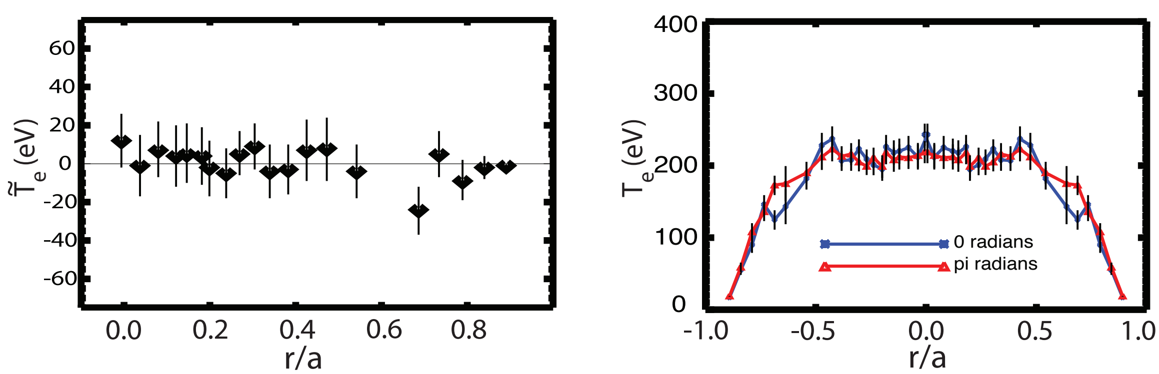

# C Complete $m = 0, n = 2$ Correlated Fluctuation Results

Below are the complete results of electron temperature fluctuations correlated to the $m = 0, n = 2$ magnetic mode during sawtooth events in 400 kA standard RFP plasmas. The left column are the fluctuations and the right column are the corresponding electron temperature profiles, $T_e = T_{e0} + \tilde{T}_{e,0,2} \cos\phi$, evaluated at $\phi = 0$ (blue) and $\phi = \pi$ (red). The time represents the time relative to the sawtooth event.

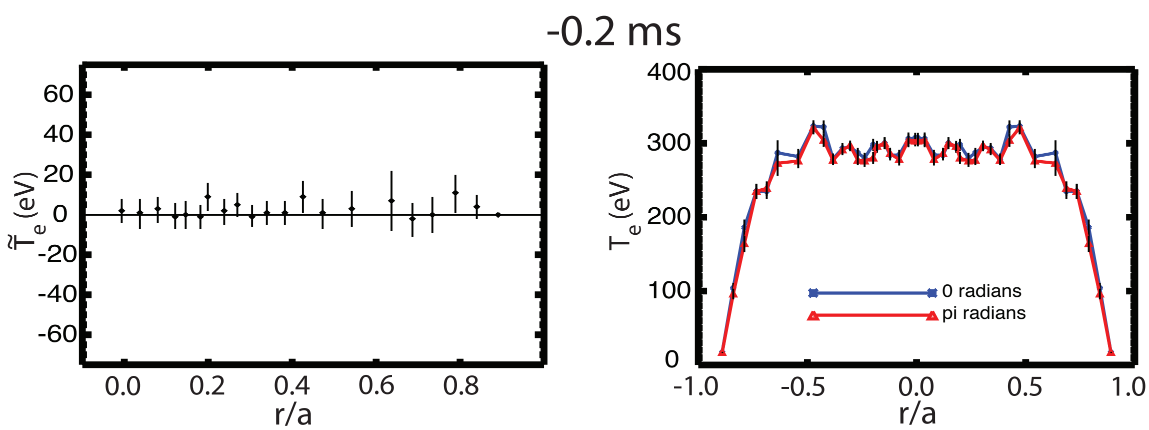

-0.10 ms

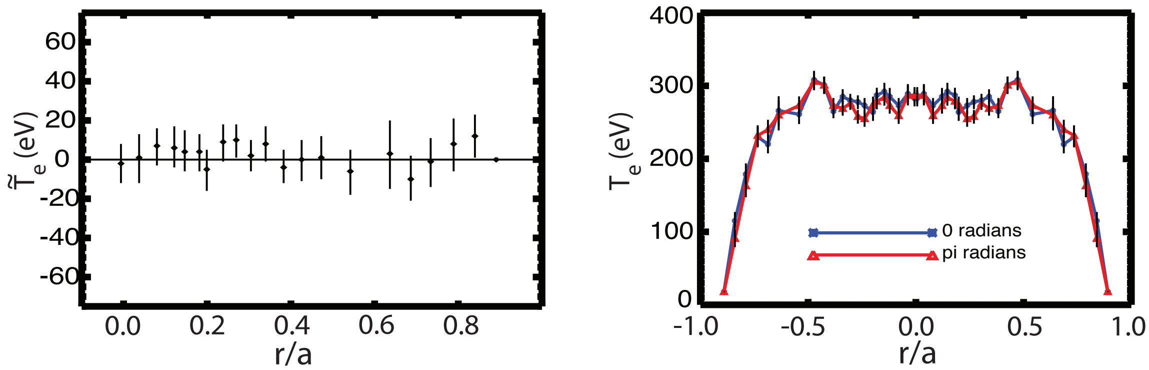


-0.05 ms

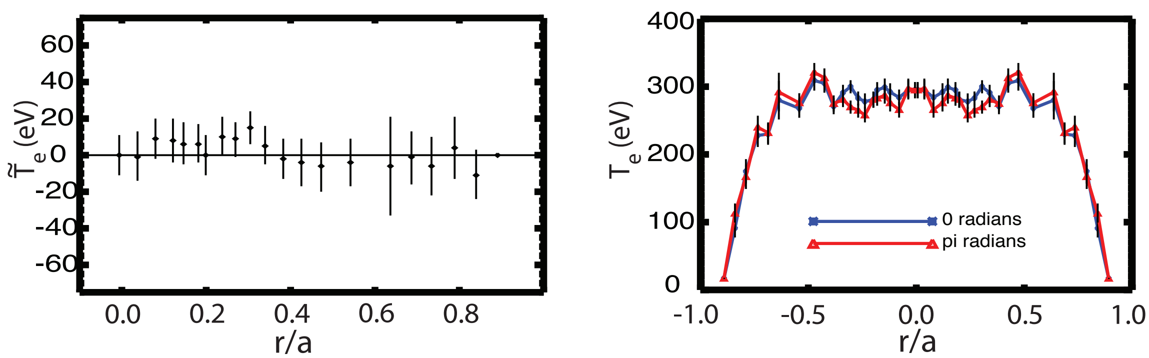


0.0 ms

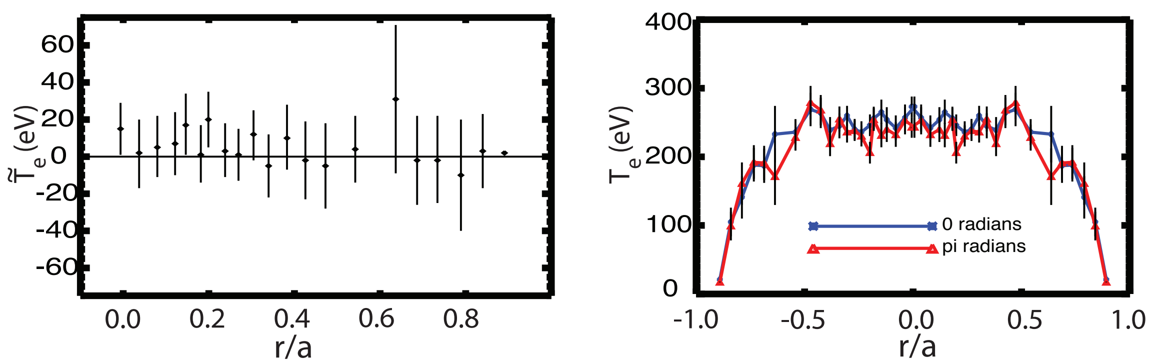

0.05 ms

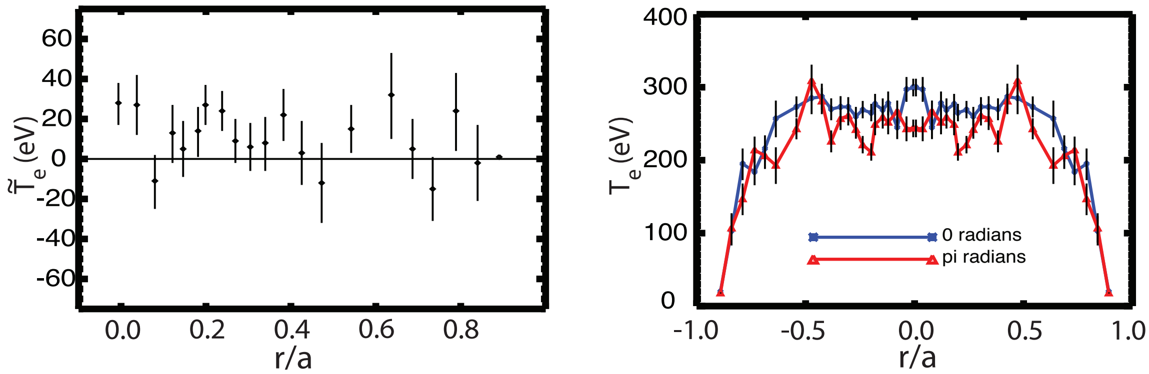


0.10 ms

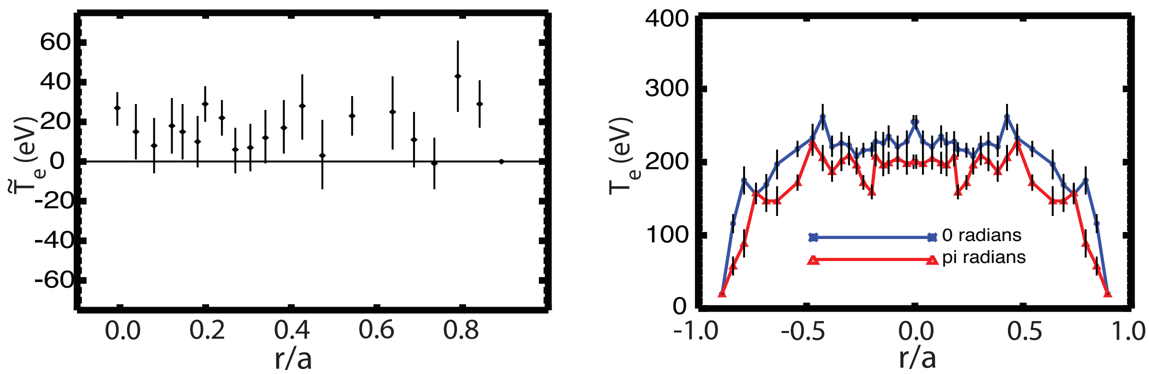


0.20 ms